Acta Cryst. (1995). B51, 447–467

The Complementary Use of X-ray and Neutron Diffraction in the Study of Crystals

BY J. L. FINNEY

Department of Physics and Astronomy, University College London, Gower Street, London WC1E 6BT, England

(*Received* 20 *September* 1994; *accepted* 23 *February* 1995)

Abstract

Neutrons and X-rays interact differently with atoms in crystals. While X-rays primarily give information on electron distributions, neutrons report on nuclear positions, and, through the spin interaction, are sensitive to magnetic structure. These and other differences have been exploited for many years in, for example, X–N difference studies and in determining magnetic structure. The major differences in available X-ray and neutron incident-beam intensities have also influenced the ways in which the two probes are exploited; not only are neutron sources inherently weaker, but this disadvantage is heightened by the weaker neutron–nucleus interaction. Advances in sources of both types, coupled with developments in instrumentation, have enabled not only the relative strengths to be exploited more effectively, but also some of the respective weaknesses in both techniques to be at least partially overcome. After outlining the main relevant advantages of X-rays and neutrons, and specifically of pulsed spallation neutron sources, this paper will discuss some of the scientific areas in which these various advantages are being increasingly exploited with advanced sources and instrumentation. Although the examples focus in particular on studies of structure and disorder in powder samples, including work at high pressures, some attention is given to hydrogen location in, and diffuse scattering from, single crystals. Finally, a personal forward look towards possible future developments is offered.

Introduction

Neutrons and X-rays interact differently with the atoms in crystals. X-rays report back on electrons. In constrast, neutrons report back on the nuclear positions, although the neutron spin means that they can also interact with the spin on an electron, making neutrons a highly appropriate probe for magnetic structural studies.

It might thus be thought that the most appropriate probe for a particular investigation could be chosen on the basis of precisely what is being determined. The situation is, however, not so staighforward. For example, consider how the probe might perturb the system under investigation. First, nucleus energy levels are $\sim 10^8$ times a typical thermal neutron energy. Thus, a normal neutron diffraction measurement will not perturb the atomic state of the system we are investigating. On the other hand, electron energy levels are of the same order of magnitude as typical X-ray energies. Therefore, in contrast with the non-perturbing neutron case, an X-ray experiment will in general change the energy levels in the system being investigated. The corrections required to the results of X-ray scattering measurements are more extensive and more complex than for neutrons. Thus, our theoretical understanding of the neutron interaction is much better, and where we are concerned to make comparisons with theory, there are thus good reasons – other things being equal – why the neutron is the probe of choice.

Unfortunately, other things are not always equal, so the choice between neutrons and X-rays is not as simple as implied above. For example, consider the relative strengths of the available sources of neutrons and X-rays. Compared with X-ray sources, neutron sources are relatively weak. This, compounded by the generally lower scattering cross-section of the neutron, often means that sample sizes for a neutron experiment must be larger than those that may be available, or that data collection times are unacceptably long. Thus, although 'theoretically' the neutron may be the most appropriate probe, the relative weakness of neutron sources has meant that a less appropriate probe has often to be used. This problem is compounded even further by the lower availability of neutron sources.

Recent years have seen a significant advance in both X-ray and neutron sources. In the former, we have now had for over 10 years storage ring sources that have allowed us to exploit the advantages of X-rays in structural and other studies. Further advances are now being realized with the coming on stream of third generation sources such as the APS at Argonne, ESRF in Grenoble, and SPRING-8 in Japan. On the neutron front, although it is generally recognized that engineering limitations will prevent reactor source development beyond the proposed Advanced Neutron Source planned for Oak Ridge, neutron production from particle accelerators has, through the experience of IPNS at Argonne, the pulsed source at Los Alamos, KENS-II at Tsukuba, and ISIS at the Rutherford Appleton Laboratory in England, demonstrated the effectiveness of an alternative line of source development through which we can expand our ability to exploit the particular advantages

of neutrons. Coupled with often major developments in instrumentation and data analysis techniques, these improvements in sources allow both enhanced exploitation of the advantages of the two complementary probes, as well as reducing some of the problems associated with each. These advances allow us to both perform existing science better, as well as new science, in both powder and single-crystal structural studies.

For example, electron storage rings produce bright highly collimated white beams covering a wide energy range up to the hard X-ray region. The brightness allow us to look at smaller samples, enables the collection of better statistics, and can begin to compensate for the normal form factor fall-off with scattering vector **Q** defined as $4\pi \sin\theta/\lambda$, where λ is the incident wavelength and 2θ the scattering angle. The hard X-rays allow us to access a wider **Q** range than from laboratory sources, as well as giving increased penetration of a sample. The availablility of an intense white beam allows us to select a narrow waveband, which not only assists us in making some of the corrections necessary in diffuse scattering studies in particular, but also, by tuning near to absorption edges, allows us to induce significant contrast between the scattering cross-sections of atoms close to each other in the periodic table. As we shall see below, this use of anomalous dispersion is enabling us to not only separate out atoms of similar atomic number, but is also beginning to allow us to perform site-specific chemistry.

Before discussing the advantages of recent developments in neutron sources, we should summarize the major advantages of neutrons in general. First, not only the wavelength, but also the energies of thermal neutrons are appropriate for condensed matter studies. Thus, although we will not consider this aspect further here, neutrons are an appropriate probe for studies of dynamics as well as structure. Secondly, as the neutron interacts with the nucleus, there is no fall-off in the scattering cross-section with increasing scattering angle (or more generally, with increasing **Q**). This enables us to make measurements with good statistics to higher resolution than is normally the case with X-rays, where the form factor fall-off can be a major problem. Furthermore, the fact that the neutron cross-section does not depend on atomic number means that neutron contrast for atoms of similar atomic number can be much greater than for X-rays. Thus, neutrons can easily distinguish Al from Si in aluminosilicates, where the X-ray contrast is very low. Moreover, different isotopes of the same element often have different neutron scattering cross-sections. This isotopic dependence can be exploited in several ways, for example, in using the H–D contrast to study structure in biological systems, or in obtaining local structural information around a specified atom. Thirdly, the neutron's magnetic moment allows it to probe both magnetic structures and excitations. Fourthly, the neutron is a weak probe. As mentioned earlier, this eases theoretical interpretation. It also allows us to probe the bulk of a material easily.

The last cited advantage of the neutron – it being a weak highly penetrating probe – is also one of its problems. As discussed above, this weakness of interaction, coupled with the relative weakness of neutron sources, sometimes prevents full exploitation of the neutron's advantages. There is thus a strong need for more intense sources of neutrons. Increases in flux of more than a factor of five or so are unlikely from reactors. However, there are major possibilities in the further exploitation of pulsed spallation sources. In these, sharp pulses of neutrons are produced when sharp pulses of protons from a particle accelerator impinge on a heavy metal target. Although the time-averaged flux of such a source is (at present) lower than that obtained from the most powerful reactor sources, within the pulse, we have a much brighter source. In most reactor experiments, a narrow waveband of neutrons is selected out by either a monochromator or a chopper, and hence only a few per cent at most of the neutrons produced are normally used. In the pulsed source, the natural pulsing, which facilitates the use of time-of-flight detection techniques to measure neutron energy, allows us to use the white beam effectively in many types of experiments.

It is perhaps useful to summarize the major differences between performing a constant wavelength (CW) diffraction measurement on a reactor neutron source, and a time-of-flight (TOF) diffraction measurement on a pulsed spallation source. In the reactor case, a narrow waveband of neutrons is selected from the incident continuous spectrum of neutrons, and the scattering from the sample – say a powder – is measured as a function of scattering angle 2θ by either a scanning detector or increasingly a multidetector covering a spread of 2θ. Intensities are then plotted normally against 2θ (*e.g.* Figs. 2–4) which can then be related to d-spacing or scattering vector **Q** *via* the Bragg equation $\lambda = 2d \sin\theta$, or the defining equation $\mathbf{Q} = 4\pi \sin\theta/\lambda$. In a pulsed source, rather than being restricted to varying only the scattering angle 2θ, the natural pulse structure enables us to take advantage of a range of wavelength λ in the incident white beam by setting a time zero for each pulse, for example, when the neutron pulse leaves the moderator surface. By measuring the time of arrival at the detector (in general, covering a range of scattering angles), and knowing the distance from moderator to each detector element, we can deduce the energy, and hence wavelength of each detected neutron from the time-of-flight. Diffraction patterns from pulsed source instruments are often initially presented as plots of intensity against time-of-flight, as in Fig. 11(*a*). This can be simply converted to a d-spacing scale (also given in Fig. 11*a*) knowing the dimensions of the instrument and its beam line. Thus, as we are in general exploiting a significant fraction of the white beam rather than monochromating it, although not as many neutrons are

produced by present pulsed spallation sources as in the most powerful reactors, appropriate exploitation of the time structure allows a much higher fraction of the produced neutrons to be used. For experiments in which monochromatic beams are essential, *e.g.* in direct geometry inelastic instruments, we can select the required incident waveband in phase with the natural pulse of neutrons produced.

Although this is not an appropriate place to discuss pulsed spallation sources in detail (see, for example, Windsor, 1981; Carlile & Finney, 1991; Finney, 1992), the major advantages that follow from the pulse structure are worth stating. These include

- high brightness and excellent signal-to-noise. These attributes allow small samples to be used, or measurements made over shorter times;
- high intrinsic resolution in both **Q** and energy. This allows subtle structural and dynamic effects to be observed;
- a wide spectral range is covered;
- data can be taken over a wide dynamic range. Thus, we can more easily see the whole picture in a single measurement, where monochromatic techniques would require scans over time, or even force the use of more than one instrument;
- as we can work with white beams, we can take a data set at a fixed scattering geometry, in effect varying wavelength λ to take data over a given range of scattering vector $\mathbf{Q} = 4\pi \sin\theta/\lambda$ at fixed 2θ instead of scattering angle 2θ. This has particular importance in working in confined sample environments, where appropriate collimation can remove the scattering from the sample environment. Examples include working under pressure and in reaction vessels;
- the natural pulse structure favours time-dependent studies;
- white beam time-of-flight techniques allow us to perform simultaneous diffraction and inelastic studies.

In this article, I propose to look at some of the scientific areas in which some of the particular advantages of X-rays and neutrons are beginning to be exploited, especially as results of advances in sources and instrumentation. The field is broad, and I will therefore of necessity limit the areas considered. Neither X–N studies of electron deformation nor of the exploitation of synchrotron sources in Laue single-crystal studies or of microcrystals will be discussed as these latter two areas are covered by Marjorie Harding in this symposium. Nor will I touch magnetic structures. Rather, after a brief example of hydrogen location in single crystals, I will concentrate on opportunities in powder work, including recent developments in work at high pressures. Finally, some recent work on diffuse scattering in single crystals will be presented, before making some summarizing comments on where the future developments may be.

Light atom location in single crystals

Neutrons are the probe of choice when trying to locate light atoms in the presence of heavy ones. In early powder work on high-temperature superconductors, neutron scattering proved its ability to locate O atoms, where the neutron contrast with the heavy atoms was much more than for X-rays. A well-established advantage of neutrons is in the accurate location of H atoms, especially if deuteration can be used to reduce the high incoherent scattering from hydrogen.

Much of the X-ray literature on hydrogen-bonding systems, in particular hydrate structures, draws inferences on hydrogen-bonding geometries from the positions of the heavy atoms, without having precise positions for the light H atoms. An example where both X-ray and neutron measurements were crucial in sorting out both hydrogen and oxygen positions – and hence molecular orientations – in a partially disordered arrangement of water molecules is provided by a study of the solvent structure in single crystals of vitamin B_{12} coenzyme (Savage, 1986*a*; Savage, Lindley, Finney & Timmins, 1987; Bouquiere, Finney, Lehmann, Lindley & Savage, 1993; Bouquiere, Finney & Savage, 1994). This work was undertaken in order to establish an accurate solvent structure in a system of biological interest, with the aim of improving our understanding of the hydration of biomolecular systems.

Although not a protein or nucleic acid, coenzyme B_{12} contains many chemical groups of relevance in both proteins and nucleic acids. The earlier work of Dorothy Hodgkin's group (Lenhert & Hodgkin, 1961; Lenhert, 1968) had established that diffraction data could be taken to very high resolution, and that crystals sufficiently large for neutron scattering could be grown. In fact, their early neutron work on a monocarboxylic acid derivative (Moore, Willis & Hodgkin, 1967; Hodgkin, 1984) was very much a *tour de force*, this then being a larger molecule than had been studied previously by neutrons. Furthermore, it was with Dorothy's strong support and encouragement – including arguing persuasively behind the scenes for the relatively large amount of neutron beam time then required – that the high-resolution coenzyme B_{12} study discussed here was initiated.

Neutron scattering data out to 0.9 Å were taken on coenzyme B_{12} crystals grown from D_2O, and neutron scattering densities of the solvent region obtained as in Fig. 1(*a*). Especially in the more solvent-disordered channel region in the centre of the figure, the data proved difficult to interpret. As the neutron scattering lengths of oxygen and deuterium are comparable, there is considerable uncertainty in assigning a particular feature to oxygen or deuterium. The problem was solved by taking X-ray data, resulting in electron-density contours as in Fig. 1(*b*), which, by comparison with Fig. 1(*a*), enabled the oxygen and deuterium density to be distinguished. From this work, a series of partially ordered solvent networks could be identified, and the detailed geometries

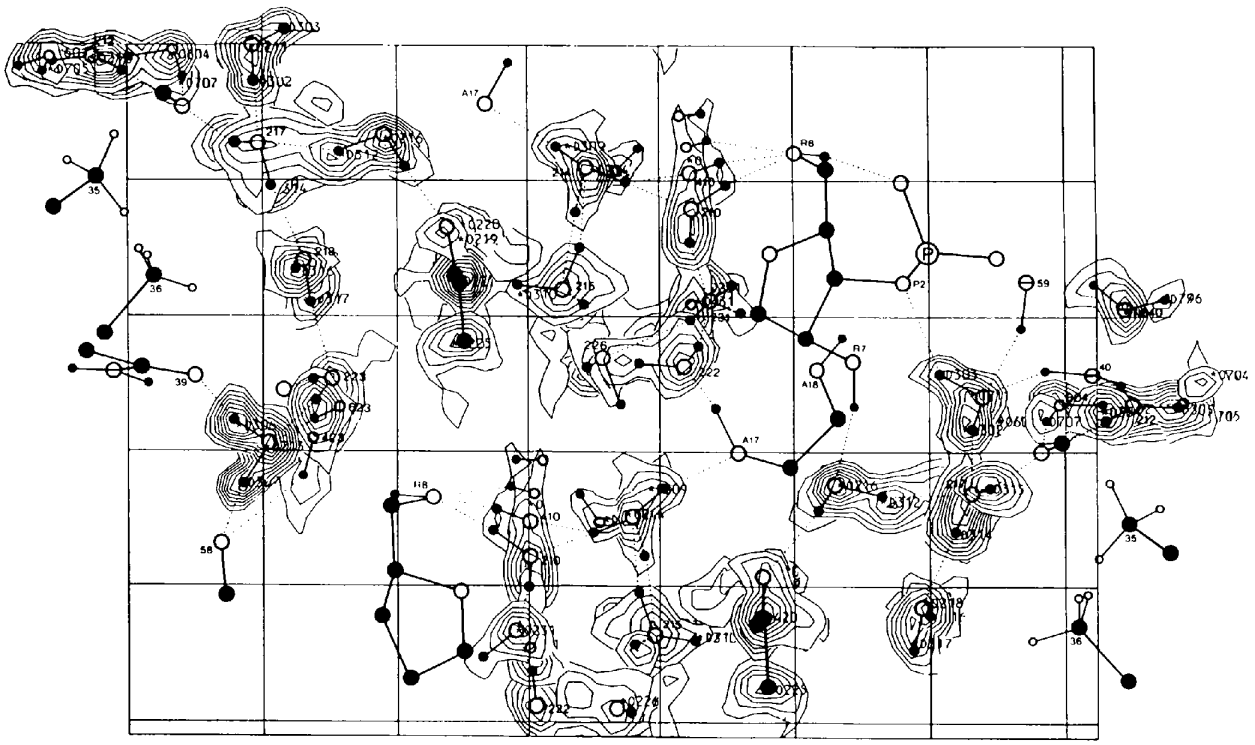

(*a*)

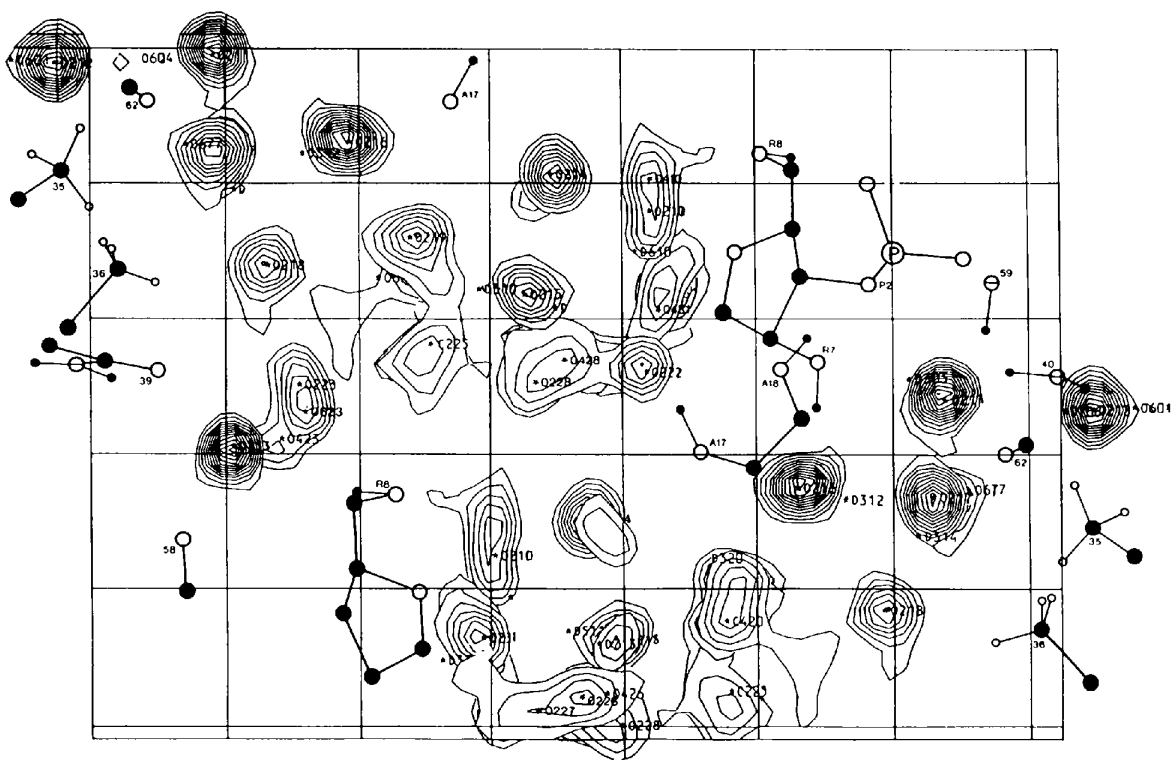

(*b*)

Fig. 1. (*a*) Neutron and (*b*) X-ray scattering density of the solvent region in coenzyme B_{12} at 279 K.

examined. As a result, some previously unrecognized structural regularities were identified (Savage, 1986*b*; Savage & Finney, 1986), which enabled us for the first time to understand the apparently irregular orientational structure of the solvent in this relatively complex hydrate. Identifying these regularities required the precise positioning of the D atoms on the water molecules; this could not have been done using the X-ray data alone.

An interesting postscript to this story is provided in Fig. 1(*c*), which shows the neutron scattering densities for the same system at low temperature (15 K). An interesting aspect of this study is that although the crystals were grown from D_2O, a considerable degree of back-exchange of hydrogen occurred. The dashed contours indicate the negative scattering length of hydrogen, and allow us to identify by inspection the hydrogen positions without having to refer to X-ray data. This illustrates some of the progress in instrumentation in the 10 years between the two studies. We should no longer automatically assume that deuteration is necessary to reduce the incoherent background, but instead note that we can work increasingly with hydrogenated samples. Not only does this remove any objections concerning possible system perturbation by deuteration, but it also reduces considerably the cost of an experiment. This is especially relevant where non-exchangeable hydrogens would otherwise need to be deuterated using synthetic chemical procedures.

High-resolution powder diffraction

The availability of higher intensity sources of either X-rays or neutrons immediately provides us with the ability to work at higher resolution. This has allowed us to make significant advances in two areas in particular, namely structure determination from powders and structure refinement, using either X-rays or neutrons, and sometimes both.

Structure determination from powders

Crystal structures are routinely solved from single crystal data. In attempting to solve structures *ab initio* from powder data serious difficulties are encountered, most of which arise from the three-dimensional intensity data being compressed into a single dimension. The resulting peak overlap introduces complications at several stages of the structure determination, for which structure factors need to be extracted for subsequent direct-methods solution. Nevertheless, if these difficulties can be overcome, then we will have a powerful technique, increasingly needed in modern materials research, where new materials are often available initially only in small quantities as powders.

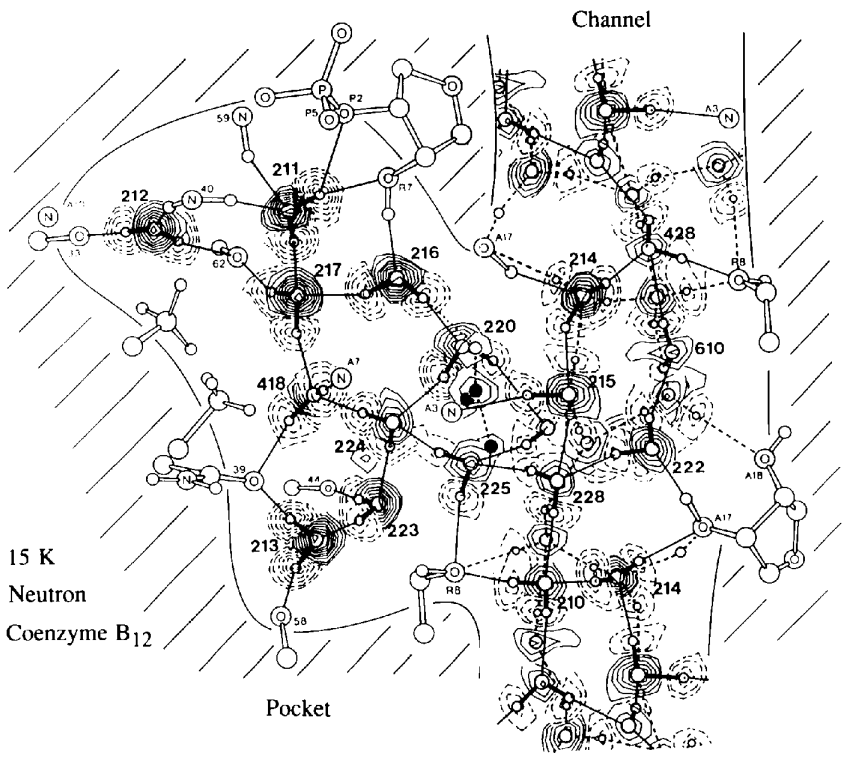

(*c*)

Fig. 1 (*cont.*) (*c*) Shows the neutron density at 15 K; negative contours show the H atoms.

The high-resolution available from both second generation X-ray synchrotron sources, and from advances in neutron sources and instrumentation, gives us significant help in various stages of structure determination. Fig. 2 shows the kind of resolution that is achievable on current synchrotron sources, with full widths at half maximum of 0.02° achievable, compared with say 0.06° for a high quality laboratory instrument. In the first step of indexing the reflections and unit-cell determination, the success of the available autoindexing programs depends very much on the availability of very accurate *d*-spacing data. These are now available from modern sources, provided of course that care is taken to remove the various sources of systematic error. Following a successful indexing, we then need to extract the maximum amount of integrated intensity data, and here again resolution is of considerable assistance. Problems will still be experienced of course with overlapping peaks, particularly those in which the overlap is complete, and no amount of additional resolution will help. Several approaches have been developed and others are under development (Pawley, 1981; LeBail, Duroy & Fourquet, 1988; David, 1990). The exploitation of maximum entropy reconstruction seems of particular promise (David, 1990), as possibly are methods being explored to make use of preferred orientation (Bunge, Dahms & Brokmeier, 1989).

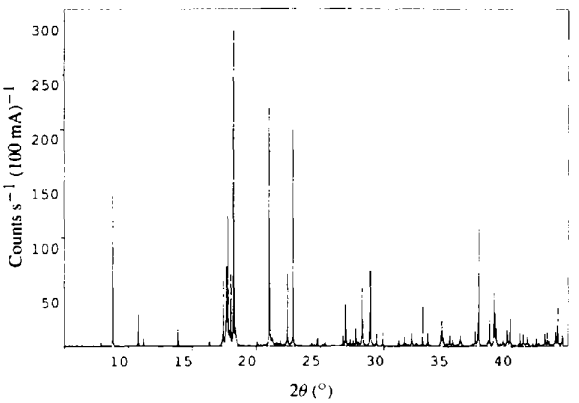

Fig. 2. A high-resolution powder pattern of $Fe_2P_2O_7$ at 45 K ($\lambda \sim 1.20$ Å), taken on beam line X7A at the National Synchrotron Light Source at BNL. Using a crystal analyser arrangement, the minimum full width at half height is 0.02° (Cheetham & Wilkinson, 1991).

Once we have an indexed pattern and have extracted intensities, then by and large structure determination follows as for a single crystal study. There are a number of successful examples in the literature, using both X-rays and neutrons. For example, the structure of a zeolite, the so-called sigma-2 clathrasil structure, was solved from synchrotron powder data (McCusker, 1988). Direct methods gave the positions of all four tetrahedral atoms, together with four of the seven O atoms in the asymmetric unit. The remaining three oxygen positions were located in the first difference Fourier map, and subsequent refinement revealed the location of the partially disordered 1-aminoadamantane. A much larger problem was the structure of the drug cimetidine, which contains 33 atoms in the asymmetric unit, and was again solved using synchrotron data (Cernik, Cheetham, Prout, Watkin, Wilkinson & Willis, 1991). The powder pattern and model fit to the determined structure are shown in Fig. 3. A number of structures have also been solved from neutron powder data, which has proved particularly useful for small organic molecules, a recent example being dimethylacetylene (Ibberson & Prager, 1995). The powder pattern measured showed substantial anisotropic line broadening. Nevertheless, the structure could be

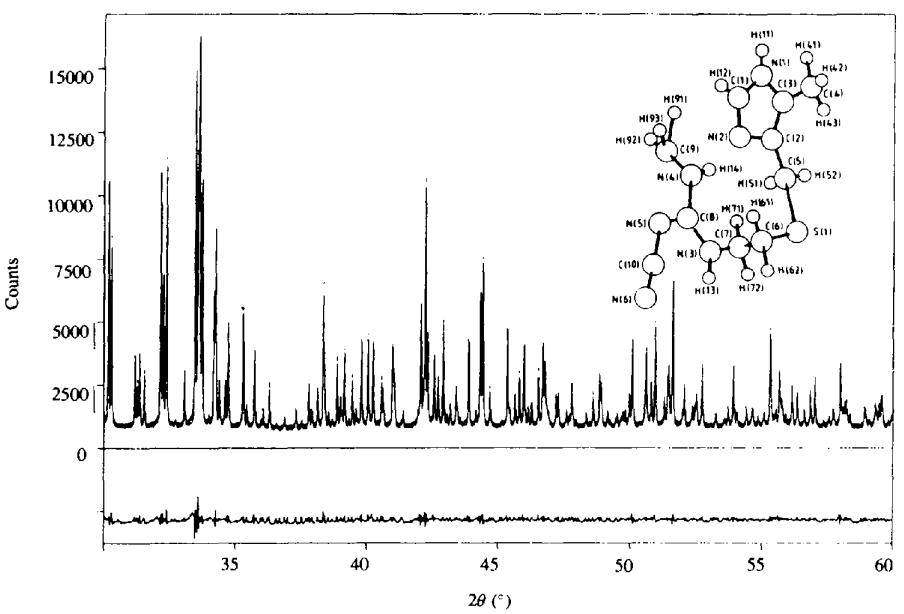

Fig. 3. The X-ray diffraction pattern from which the structure of the drug cimetidine was solved at the Daresbury Laboratory (Cernik, Cheetham, Prout, Watkin, Wilkinson & Willis, 1991).

solved and additional information on the disorder in the structure obtained in the subsequent refinement.

Apart from what we might call standard structure determination from powders, there is significant potential to exploit the particular strengths of X-rays and neutrons in the solution procedure. An obvious example is the use of X-rays to solve the 'heavy atom' framework of a structure, then making use of neutron data to locate the light atoms. An example is the structure of sodium methyl (Weiss, Corbelin, Cockcroft & Fitch, 1990*a*,*b*), with ten atoms in the asymmetric unit. One would also expect exploitation of both neutron isotope substitution and X-ray anomalous dispersion in solving the phase problem. Although the latter is used extensively in protein structure determination from single crystals, little seems to have been done so far along similar lines in *ab initio* structure solution from powders. We might note here that the problems that have so far been tackled are relatively small, and therefore ought to be amenable to direct-method solutions of the phase problem. The possibility of exploiting anomalous dispersion for phasing should, however, be borne in mind.

Structure refinement

High resolution allows us access to reliable data on more reflections. As each reflection is a Fourier component of the structure, we can therefore expect to be able to perform higher quality refinements, both of structure and of various types of disorder. We can also begin to carry out good quality refinements from more complex structures, and to see more subtle effects. Access to higher-energy X-rays from synchrotron sources, and to higher energy neutrons from spallation sources, enables us to increase the momentum transfer range of our data, and hence extend our measurements to even higher real space resolution.

Both X-ray and neutron work have demonstrated the potential of high resolution in structure refinement. Here, the Rietveld profile refinement method (*e.g.* Young, 1993), in which the scattering pattern generated by a model structure is fitted to the measured powder pattern, has led to major advances in powder crystallography. An example of an X-ray refinement is that of the aluminophosphate framework structure VPI-5, the observed, calculated and difference profiles being shown in Fig. 4. Interesting results from this refinement (McCusker, Baerlocher, Jahn & Bülow, 1991) included the conclusion that one third of all the Al atoms are octahedrally coordinated to four framework O atoms and two water molecules, and also that there is a beautiful ordered water structure within the 18-ring channel. The octahedrally coordinated Al atoms link to one another *via* a hydrogen-bonded chain of water molecules which form a triple helix. This water structure has important implications for our understanding of the synthesis process. Without the information content of the high-resolution powder pattern made possible by the use of synchrotron radiation, this important result would not have been obtainable.

The use of synchrotron radiation, however, cannot fully compensate for one of the major deficiencies of X-rays, namely the fall-off with scattering vector of the form factor. Thus, although the VPI-5 data included sharp peaks with measurable intensity at high angles, the quality of the data of necessity will fall off as higher momentum transfers are reached. This is obvious from Fig. 4, where there is a clear reduction in intensity at high angle, yet it is in this high-angle region that the powder peaks become more dense, and hence it is here that we would like the data quality not to deteriorate. As stated earlier, this problem does not occur with neutrons, where the form factor is constant with the scattering vector. There are two further advantages of neutrons which should also be borne in mind at this point. First, while X-ray scattering factors vary with atomic number, and therefore may differ by up to two orders of magnitude between elements, neutron scattering lengths all fall within a small range, only falling outside $(-10$ to $+10) \times 10^{-15}$ m in rare cases. This lack of extreme contrast between different elements tends to result in quantitatively better refinements from neutron data than from X-rays. In particular, for systems which may contain atoms with X-ray scattering lengths over a wide range, the strong contrast will make seeing the light atom more difficult, and refined parameters will tend to be less reliable. We have already mentioned the location of hydrogen in single crystals. Another example of some importance is the high-temperature superconductors. In these systems, important atoms such as oxygen scatter X-rays much more weakly than the metal atoms found in the various types, while with neutrons the scattering lengths are much more even. It is probably for this reason – perhaps in conjunction with the wider **Q** range accessible for neutrons – that much of the early pioneering work on the ceramic superconductors was

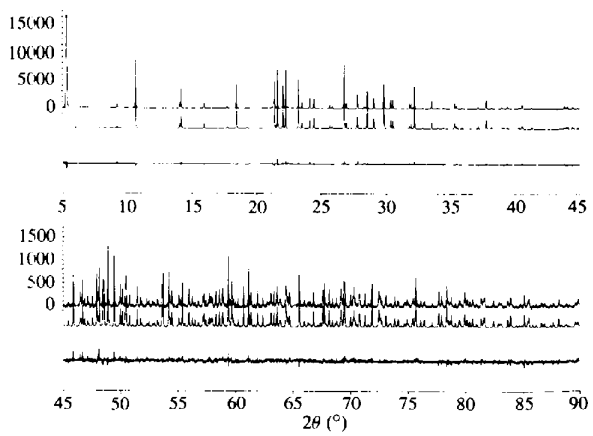

Fig. 4. The observed calculated and difference profiles for the Rietveld refinement of VPI-5 (McCusker, Baerlocher, Jahn & Bülow, 1991). Note the scale expansion of the higher angle data.

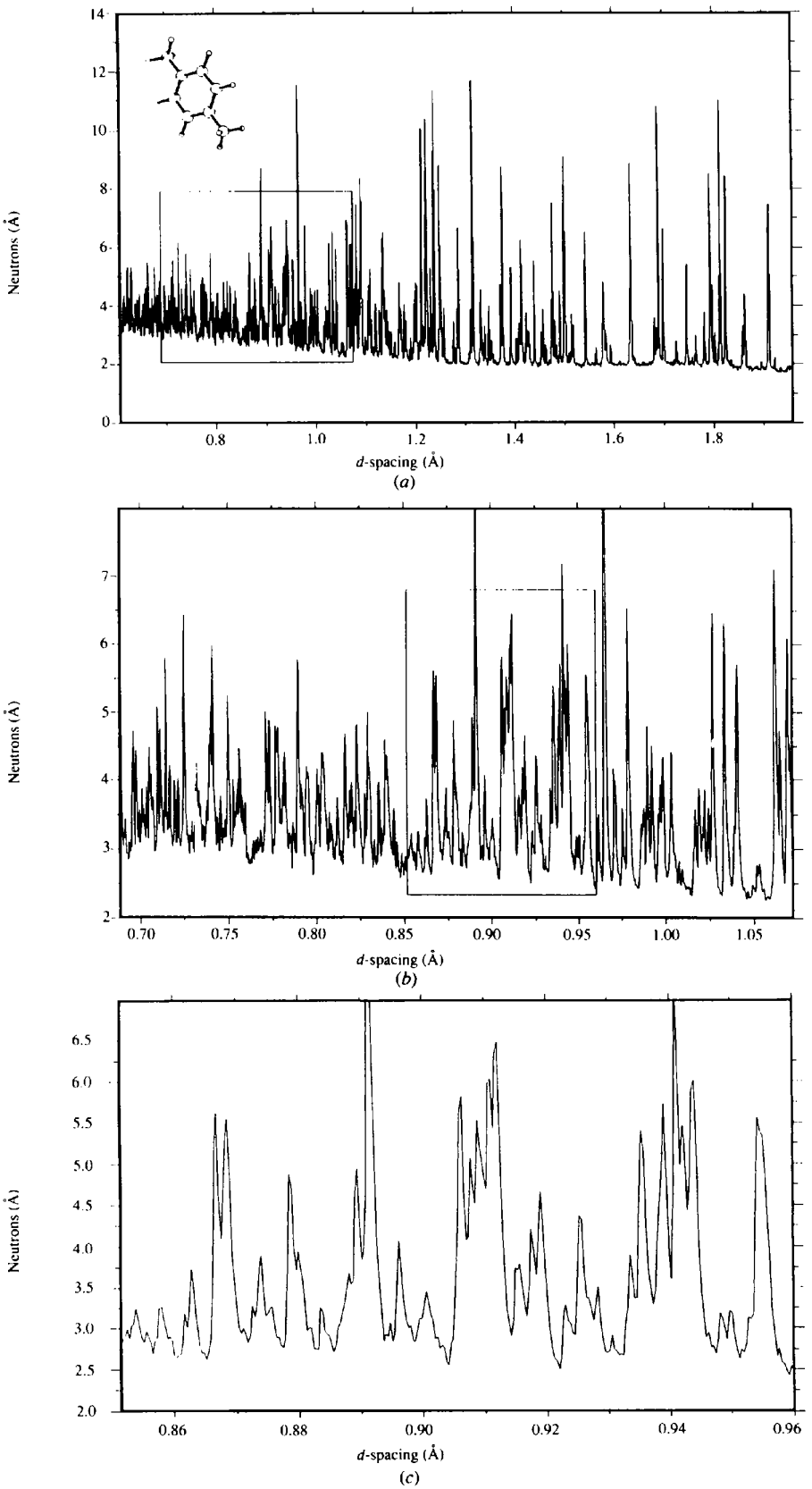

Fig. 5. (*a*) A high-resolution neutron powder pattern of *p*-xylene taken on HRPD at ISIS, illustrating both the very high and constant resolution, and the band width available in a single measurement. (*b*) and (*c*) show the regions framed in (*a*) and (*b*), respectively, enlarged.

with neutron scattering. The second neutron advantage, which comes from the use of time-of-flight techniques applied to the white neutron beams obtained from pulsed spallation neutron sources, is the fact that the resolution, defined as $\Delta d/d$ (where the d-spacing d is defined through the Bragg equation $\lambda = 2d \sin\theta$), is not only high ($\sim 4 \times 10^{-4}$ on the high-resolution powder instrument at ISIS), but it is essentially constant with the scattering vector. In contrast, although we can also obtain high-resolution powder lines from a reactor neutron source, maximum resolution is achieved only over a limited d-spacing range centred on the monochromator take-off angle. In a synchrotron experiment, high resolution requires the use of monochromatic radiation and, therefore, an angle-dispersive data collection mode. Thus, there will be a geometrical contribution to the resolution, which will result in lower resolution at the lower d-spacings.

Fig. 5(*a*) shows the kind of high-resolution data that can be obtained from the high-resolution powder diffractometer HRPD at the ISIS pulsed neutron source. That the data at low d-spacings is real is illustrated by the two magnified sections shown in Figs. 5(*b*) and (*c*). The high and constant d-spacing resolution allows us to obtain high quality data on a very large number of Fourier components of the structure. We should, therefore, expect to be able to obtain from such powder data structural refinements of very high quality indeed.

In fact, it is now possible to obtain from powder experiments data that is of single crystal quality. Thus, not only can we obtain very good structural information, but also we can refine, for example, disorder parameters with good confidence. One of the early demonstrations of the power of high-resolution neutron powder diffraction was the refinement of the anisotropic temperature factors of benzene (David, 1990). Table 1 shows the results obtained, and compares them with those obtained from single-crystal data (Jeffrey, Ruble, McMullan & Pople, 1987). Comparing the two sets of results shows that the powder data indeed produces essentially the same results as the single crystal. The estimated standard deviations from the powder data are perhaps three times larger than from the single-crystal results. However, the single-crystal data took 3 weeks to collect, while the powder data was taken in an overnight run. Thus, when considering the use of an expensive resource such as neutrons, it is as well to consider the use of powders where the additional small gain in precision may not be necessary – as indeed it was not in this case, where the data were used to discriminate between different lattice dynamic models. The powder was as capable as the single-crystal data of discriminating between the models tested.

There is an increasing number of examples of such high-quality neutron refinements. Recent examples include the biologically important molecule dopamine, where 107 parameters were refined using 5366 profile

Table 1. *Anisotropic temperature factors* (10^4 Å^2) *for deuterated benzene*

	B_{11}	B_{22}	B_{33}	B_{23}	B_{13}	B_{12}
Time-of-flight powder neutron diffraction (4 K)						
HRPD; $0.281 < \sin\theta/\lambda < 0.824$ Å^{-1}						
C(1)	77 (7)	42 (6)	87 (7)	1 (5)	5 (5)	−3 (4)
C(2)	71 (7)	58 (7)	68 (6)	9 (4)	26 (5)	12 (4)
C(3)	83 (7)	57 (7)	92 (7)	0 (5)	18 (5)	−1 (4)
D(1)	218 (8)	121 (7)	267 (9)	19 (5)	22 (6)	31 (5)
D(2)	170 (8)	212 (8)	225 (9)	−2 (6)	120 (6)	33 (5)
D(3)	241 (9)	155 (8)	214 (8)	75 (6)	66 (7)	−20 (5)
Single-crystal neutron diffraction (15 K)						
BNL – four-circle; $\lambda = 1.0499$ Å, $0.403 < \sin\theta/\lambda < 0.780$ Å^{-1}						
(Jeffrey, Ruble, McMullan & Pople, 1987)						
C(1)	79 (2)	67 (2)	88 (2)	4 (1)	7 (2)	6 (2)
C(2)	74 (2)	81 (2)	79 (2)	0 (2)	17 (2)	9 (2)
C(3)	81 (2)	75 (2)	82 (2)	10 (1)	14 (2)	−3 (2)
D(1)	224 (2)	114 (2)	239 (3)	12 (2)	25 (2)	46 (2)
D(2)	183 (2)	204 (3)	208 (3)	−8 (2)	88 (2)	35 (2)
D(3)	214 (3)	171 (2)	199 (3)	58 (2)	61 (2)	−18 (4)

points (David, 1993). It is for molecules such as this that high-resolution neutron diffraction seems to have major potential in the pharmaceutical industry. X-rays can take us some of the way, but in cases such as this where the hydrogen location is potentially crucial in understanding a drug–receptor interaction, neutrons have a clear advantage. Also in pharmaceuticals, the efficacy of a drug often varies with its formulation. Powder work has considerable potential here in helping us to understand the subtle structure–activity effects responsible for the efficacy variations.

A third recent example is of fundamental interest and demonstrates the ability of high-resolution powder neutron diffraction to provide a valuable insight into a subtle structural problem. In this case of hexamethylbenzene, the problem is the perennial one of the nature of the benzene ring. The planarity of the hexamethylbenzene molecule in the ambient-temperature triclinic structure had been demonstrated by Kathleen Lonsdale as early as 1929 (Lonsdale, 1929). It is, therefore, somewhat surprising that below a phase transition at 116 K the structure seems to be pseudo-cubic, apparently at variance with the requirements of molecular planarity. The HRPD neutron measurements (David, 1992) indicate a cubic cell, but crucially reveal a small rhombohedral distortion in this phase. The small lattice strain ($\varepsilon = 1.35 \times 10^{-3}$) is difficult to detect on other medium-resolution diffractometers. The structure is indeed found to be rhombohedral and has a well defined two-dimensional structure, with the molecule lying in the *ab* plane. In fact, within this structure, symmetry permits a crown configuration, thus allowing a small departure from ideal planarity. However, results from an unconstrained refinement give a puckering angle of carbon in the benzene ring of 0.00 (3)°; the benzene ring is thus precisely planar to within experimental error. The puckering angle of the methyl carbon, on the other hand, is 0.96 (3)°, a small but significant departure from planarity. The precision and accuracy of these results

for hexamethylbenzene provide highly reliable data for theoretical chemistry calculations.

Buckminsterfullerene C_{60} provides a further illustration of the power of high-resolution neutron powder diffraction. Considering first the low-temperature structure, and using the notation 6:6 and 6:5 bonds to denote C—C bonds fusing two hexagons and a hexagon and pentagon, respectively, the bond lengths obtained from the Rietveld refinement could clearly be divided into five short 6:6 bonds [1.391 (18) Å] and ten long 6:5 bonds [1.455 (12) Å; (David, Ibberson, Matthewman, Prassides, Dennis, Hare, Kroto, Taylor & Walton, 1991)]. This observation confirmed *ab initio* calculations (Lüthi & Almlöf, 1987) that the C_{60} unit has a significantly anisotropic electron distribution. The pentagons, which consist of long bonds, constitute an electron-poor region, while the 6:6 bonds are short and of higher bond order with significant π-electron density. When we look at the packing of the C_{60} units in the structure, we find that the electron-rich 6:6 bonds are aligned optimally over the electron-deficient pentagons, with the C_{60}–C_{60} orientational ordering being fully characterized by just the one packing motif, as illustrated in inset (*a*) of Fig. 8.

Fig. 6 shows the cubic lattice parameter of C_{60} as its temperature is lowered from room temperature. Each data point took ~ 10 min to collect, and the error bars are smaller than the circles surrounding each plotted point. In addition to confirming the expected first-order phase transition at 260 K, there is also clear evidence of a continuous phase transition at 86 K. The interpretation of the diffraction data (David, Ibberson & Matsuo, 1993) is shown in Fig. 7. In the high-temperature f.c.c. phase above 260 K, the C_{60} molecules are orientationally disordered, undergoing continuous reorientation. Below 260 K, the diffraction data are consistent with a uniaxial jump reorientation principally about a single ⟨111⟩ direction, while in the lowest temperature phase ($T < 86$ K), rotational motion is frozen, although a small amount of static disorder still persists.

The data are even sufficient to enable us to characterize this subtle disorder. In addition to the idealized near-neighbour orientation shown in inset (*a*) of Fig. 8, a second less-energetically favourable orientation can be identified. In this configuration, which is illustrated in inset (*b*) of Fig. 8, 6:6 bonds are aligned over hexagons of a neighbouring C_{60} molecule. The occupancy of the preferred configuration (*a*) obtained

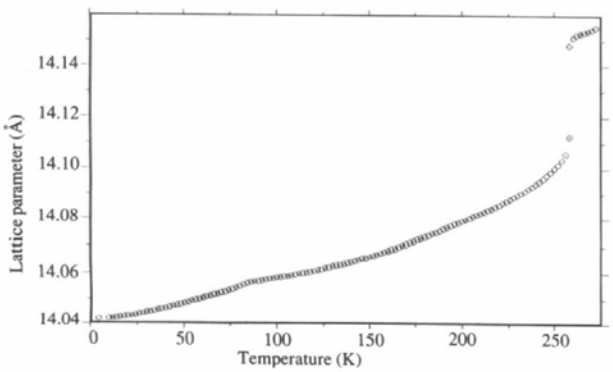

Fig. 6. The temperature variation of the lattice parameter of C_{60}, showing transitions at around both 260 and 86 K.

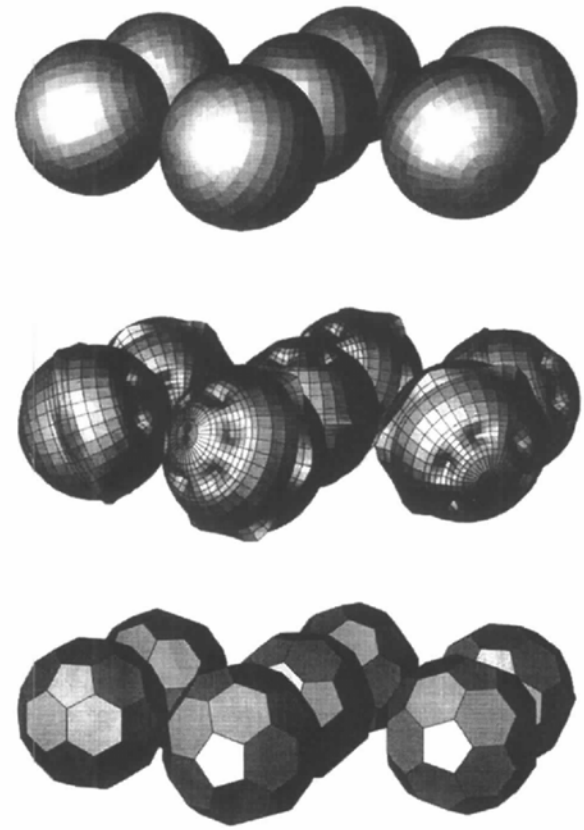

Fig. 7. A model of the dynamics of C_{60}, consistent with the powder data. Above around 260 K, molecules appear to rotate with no preferred axis (right). Below the upper transition, rotation becomes restricted to a single axis (centre), while below *ca* 86 K the low-temperature structure is adopted (left).

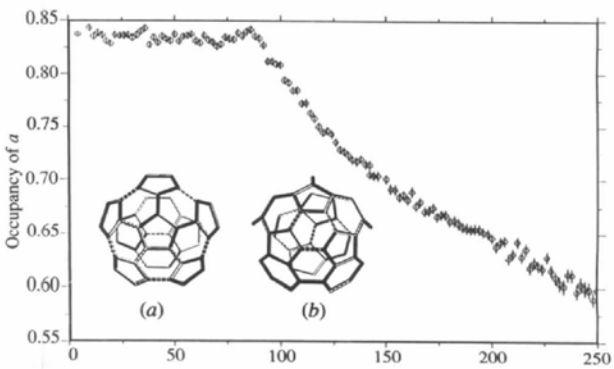

Fig. 8. The fractional occupation of the favoured local configuration (*a*) increases to 0.833 ($\frac{5}{6}$) as the temperature falls to 86 K. Below this temperature, the two configurations (*a*) and (*b*) are frozen with relative occupancies 5:1, respectively.

from the powder diffraction data is shown in Fig. 8, and shows a continuous increase to a value of 0.833 (or a fraction of five sixths) at the lower phase transition temperature. We thus have an interpretation of this 86 K phase transition in terms of a glass transition, at which the disorder of the two alternative orientations of neighbouring C_{60} molecules freezes in (David, Ibberson, Dennis, Hare & Prassides, 1992). Thus, below 86 K, rotational motion appears to have ceased, although a small amount of static disorder still persists and can be characterized by high-resolution powder neutron diffraction.

Finally, we can also use these data to evaluate the departure from isotropic scattering of the C_{60} molecule in the disordered high-temperature phase. It might be anticipated that no deviations from isotropic scattering would be expected because in a powder pattern, reflections with the same wavevector magnitude overlap, and thus diminish our ability to resolve directional information. Although this is indeed the case, we find that deviations from spherical scattering density can be refined from powder data which are consistent with results obtained from single-crystal synchrotron data, as shown in Fig. 9. Although the powder data were obtained over a similar **Q** range, the data are, not surprisingly, of poorer resolution than the single-crystal results. Nevertheless, the important features are evident from the powder data, confirming the power of the Rietveld method when combined with high-resolution data.

These examples of work on C_{60} underline the power of high-resolution neutron measurements, emphasizing the impressive amount of – sometimes quite subtle – structural information that is contained in such a diffraction pattern. Rapid data collection coupled with high resolution has enabled subtle aspects of the 86 K transition to be observed, and the structural nature of the orientational glass transition elucidated. Furthermore, analysis of the cubic lattice constant has enabled relaxation times and the reorientational activation energy of the two C_{60} orientations to be determined (David, Ibberson & Matsuo, 1993). Despite the fact that powder measurements collapse three dimensions of diffraction data onto one dimension, an impressive amount of structural information can still be extracted from high-resolution work. This applies to both X-ray and neutron measurements, although the specific advantages of neutrons – in particular, the lack of form factor fall-off with **Q** and the ability with pulsed spallation neutrons to measure over a wide range of *d*-spacing with constant high resolution – strongly favour neutrons for many problems of both fundamental scientific interest and potential technical exploitation.

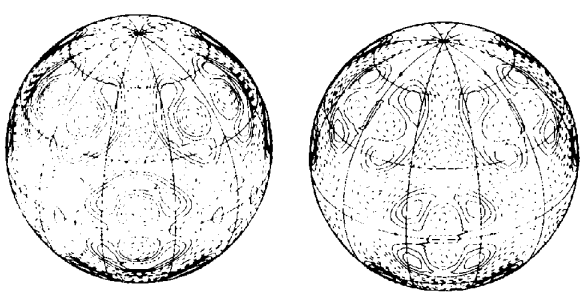

Fig. 9. The orientational distribution function viewed down one of the ⟨111⟩ directions for C_{60}, in the disordered phase at 270 K, determined from HRPD neutron data, together with the comparable results obtained from single-crystal X-ray synchrotron data. Full and dotted lines correspond to positive and negative contours, respectively.

Total scattering measurements

The experiments discussed so far have been restricted to the measurement of Bragg intensities, which yield a time-averaged structure. A model of the crystal structure is refined in order to fit the observed (Bragg) diffraction pattern. However, if we measure the total diffraction pattern, we can obtain, by Fourier transform, information on the instantaneous distribution of atoms to yield what is in essence a one-dimensional Patterson map. One type of experiment that considers non-Bragg scattering is the study of diffuse scattering in single crystals, an area which is discussed in a subsequent section below. In the context of powder diffraction, however, it is useful to discuss the type of experiment that is performed when making a structural study of a liquid or amorphous material. As in a powder measurement, full three-dimensional structural information is lost. However, by obtaining information on the radial distribution function by Fourier transforming the total diffraction pattern, we can address important questions concerning the details of inter- and intramolecular *distances*. The fact that the instrumentation used for liquids and amorphous diffraction measurements emphasizes high momentum transfer means that information on interatomic distances is potentially available to a higher real space resolution than normally obtainable from a classical crystallographic (powder or single-crystal) study.

The information available from a total diffraction measurement is normally presented as a radial distribution function, or pair correlation function $g(R)$, which gives us the probability of finding an atom at a distance R from any other atom. Taking again as an example C_{60}, the measured structure factor taken on the ISIS pulsed spallation neutron source is shown in Fig. 10(*a*). Two points might be noted here. First, the resolution in **Q** space is modest, far *lower* than we obtain from an instrument specifically designed for powder diffraction. Secondly, the wavevector range accessed is much *higher* than that obtained in a normal powder measurement: structural information can clearly be seen in the data up to $\mathbf{Q} = 40\ \text{Å}^{-1}$, the limit of the plot shown, equivalent to a *d*-spacing of 0.16 Å.

Transforming these data into real space, we can draw several conclusions of interest. First, concentrating on the

first peak in the radial distribution function (Fig. 10*b*), there is a clear asymmetry, from which can be extracted using Bayesian analysis techniques two distinguishable C—C bond lengths. We recall from the earlier discussion that two distinguishable bond lengths were obtained from powder crystallography measurements, so these results would appear to suggest nothing new. However, referring to Table 2, where the two bond lengths and their uncertainties are compared between the total diffraction and powder results, we see that the precision of the distances is significantly greater from the total diffraction measurement, even though these data were taken at a higher temperature. Thus, this approach is able to give precise information on interatomic distances. The total diffraction data can be viewed in other ways also. For example, looking at the pair correlation function for the intramolecular structure shows there is essentially no difference in the molecular structure of C_{60} between room temperature and 20 K (Fig. 10*c*). There is, however, a very pronounced difference between the intermolecular radial distribution functions at room temperature and 20 K. The room-temperature results agree well, although not exactly, with a model involving the close packing of spherical shells of scattering density. The 20 K intermolecular function indicates orientational ordering, confirming that a structural phase transition has indeed occurred.

Table 2. C—C *bond lengths* (Å) *in* C_{60}

Technique	6:6 bond	6:5 bond
Total scattering (room temperature)	1.377 (7)	1.458 (3)
Powder diffraction (5 K)	1.391 (20)	1.455 (12)
NMR	1.400 (15)	1.450 (15)
Ab initio	1.390	1.450

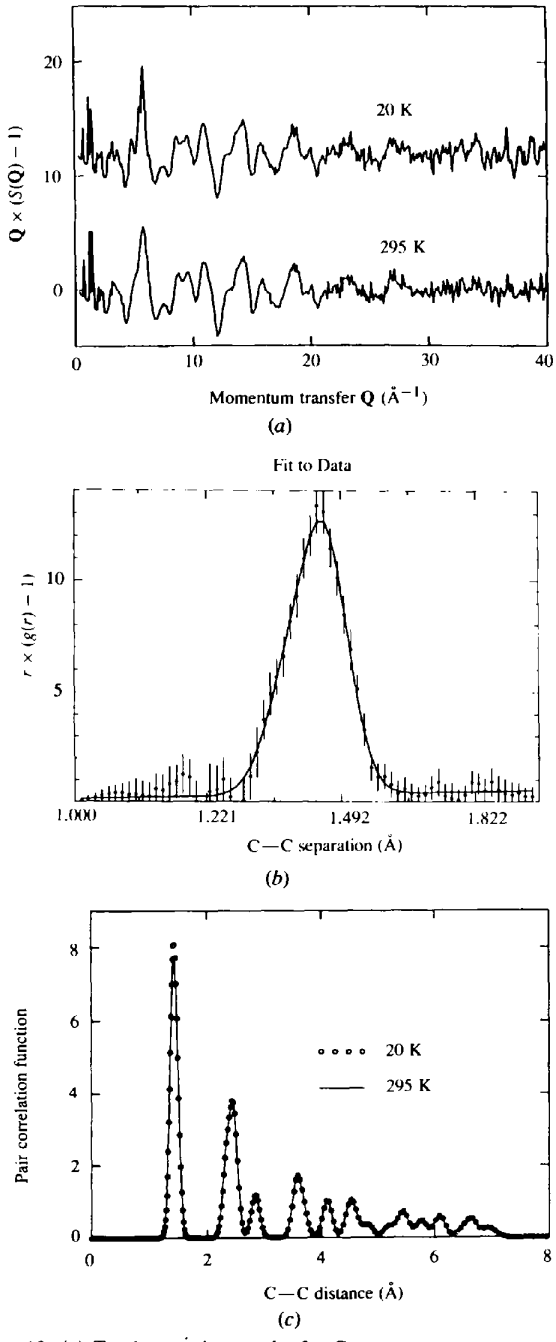

Fig. 10. (*a*) Total scattering results for C_{60} at room temperature and 20 K. (*b*) The first peak in the real space pair correlation function of C_{60}. The peak asymmetry allows two different C—C distances to be extracted. (*c*) Calculated pair correlation for the intramolecular C_{60} structure; the results for the two temperatures are essentially the same.

Although we have used C_{60} to illustrate the type of information that can be obtained from total diffraction measurements, there are clearly potential applications in many other systems where information on short-range structural distortions is needed, and that information cannot be extracted from the average structure obtained from straight crystallographic studies. One further example concerns the copper–oxygen layer in the prototype high-temperature superconductor $LaCu_2O_4$ (Billinge & Egami, 1992), which the crystallographic results tell us is planar. When we compare the pair distribution function calculated from the crystal coordinates with the measured functions from total diffraction measurements both above (50 K) and below (10 K) the superconducting transition, we find there are clear differences both from the 'average' structure provided by crystallography, and between the superconducting and non-superconducting states. The local structure is thus considerably different from the average crystallographic structure, and changes in the local structure can be associated with the onset of superconductivity. Structural modelling indicates that the observed differences can be explained partly by O atoms being displaced by small amounts (~ 0.12 Å) perpendicular to the CuO_4 plane, giving rise to plane buckling. There are also in-plane displacements which appear to be ordered in a way that suggests collective rotations of the CuO_4 squares about the [001] axis. This information is potentially of importance to our understanding of the superconducting

mechanism; it required total diffraction measurements using neutrons to obtain it.

Site ordering

We can perhaps distinguish two kinds of site-ordering problems. First, when a site is only partially occupied, we can refine its occupancy, given adequate data. Examples abound in hydrate systems, where the ability of the water molecule to both accept and donate two hydrogen bonds leads to rich disorder behaviour, *e.g.* in the ice phase diagram. Secondly, a site may be occupied by more than one kind of atom. Examples include aluminosilicates, where a framework site may be occupied by either an Al or Si atom, and systems in which different charge states of the same atom may occupy a given site.

Of the first – site occupancy problems – I will say little, except to comment on the often-encountered problem of correlation between temperature factor and occupancy, preventing a complete solution. With additional data, this correlation can be broken, and the increased range of *d*-spacing available both in the X-ray and neutron cases is likely to increasingly help us obtain improved occupancy information. An example from the ice-phase diagram concerns the hydrogen ordering in ice IX. Because we are interested in hydrogen positions, this is clearly a neutron problem. Using D_2O, data on the phase both (*a*) under pressure and (*b*) after recovery to ambient pressure at liquid nitrogen temperature were collected on the D1A diffractometer at the ILL, out to *d*-spacings of around 1 Å (Londono, Kuhs & Finney, 1993). As the correlation between temperature factors and the occupancy parameters prevented convergence of the refinement, advantage was taken of the wider *d*-spacing range available on the ISIS-pulsed spallation source, and the data on the recovered phase taken on the high-resolution powder diffractometer HRPD. These additional data allowed the deuteron occupancies to be refined satisfactorily, with occupancies consistent with – although of significantly better precision than – earlier single-crystal results. In addition to illustrating the use of the wider *d*-spacing range increasingly available on advanced sources to refine partial occupancies, this provides a further example of the ability of powder methods to obtain data of single-crystal quality.

Of probably greater interest, especially in modern materials science, is the second type of site-ordering problem where a given site can be occupied by more than one type of species. It has been realized for decades that the different contrasts produced by X-ray and neutron measurements can be exploited to increase the contrast between two atom types that may occupy a given site. A classical case is that of aluminosilicates, in which the ordering of aluminium and silicon on a given site is difficult to obtain by X-rays due to the similar X-ray scattering power of the two atoms. As the situation is different for neutrons, neutron scattering is, therefore, the method of choice in determining, for example, the ordering of Al on framework sites.

An example of geological interest, in that the relative occupancies of the two atoms may be an appropriate candidate for a geothermometer/geobarometer on natural

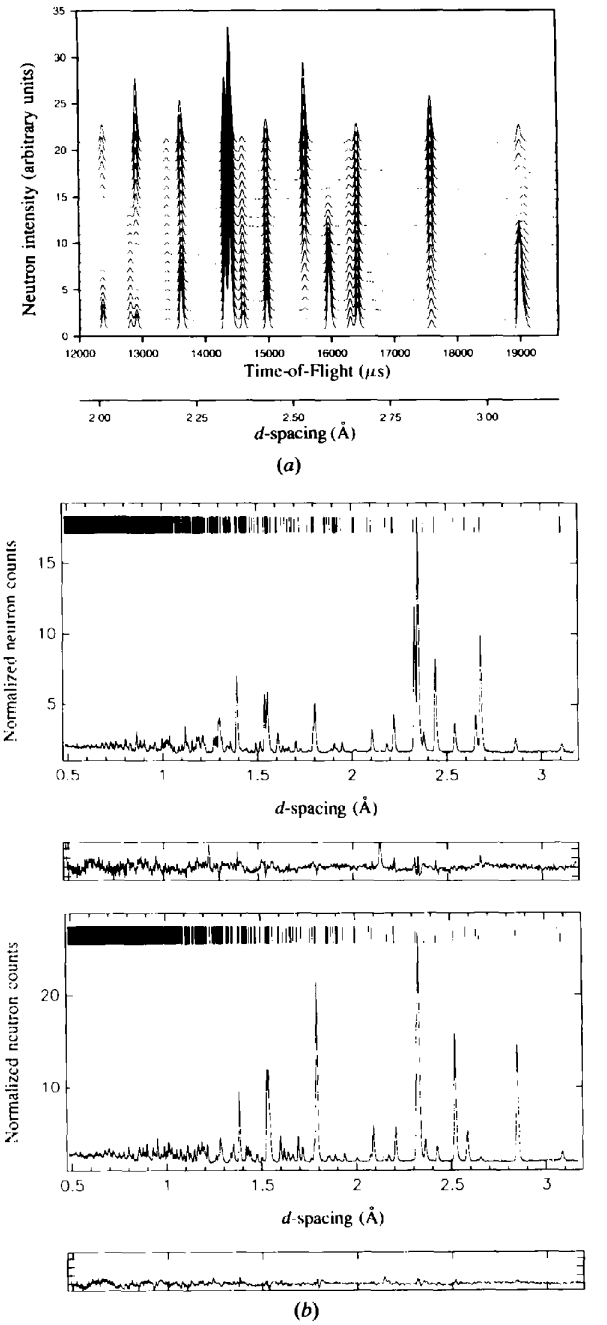

Fig. 11. (*a*) Simulation of the diffraction patterns due to cation ordering in (Fe,Mn) olivine, moving from all Mn in the *M*1 site (bottom trace) to all Fe in the *M*1 site. (*b*) shows the experimental neutron powder pattern for 0.3 Mn (top) and 0.7 Mn (bottom); there are clear differences in the intensities of various peaks. Note the horizontal scale in time-of-flight can be converted to the *d*-spacing scale knowing the instrument geometry, as discussed in the *Introduction*.

samples, is the ordering of Fe and Mn in (Fe, Mn) olivines (Knight, Henderson & Wood, 1995). Fig. 11(*a*) shows in simulated powder patterns the large differences to be expected as the $M1$ site occupancy goes from all Fe to all Mn in a 50:50 (Fe,Mn) olivine. The changes with occupancy are significant. Fig. 11(*b*) shows powder diffraction data for 30% and 70% Mn olivines, and shows clear differences between the patterns from which can be refined the relative site occupancies as functions of the Fe:Mn ratio.

Clearly, if we can by some means introduce a significant difference in the scattering powers of the candidate occupants of a site, high-resolution powder diffraction is potentially capable of determining the relative occupancies. One way of doing this with neutrons is to take advantage of the fact that the neutron scattering length of an element can vary with isotope. An example of such an isotope substitution study is the determination of the substitutional mechanism of Ca in the $YBa_2Cu_4O_8$ superconductor (Fischer, Kaldis, Karpinski, Rusiecki, Jilek, Trounov & Hewat, 1993). Earlier work had shown that in Sr doping, the strontium apparently replaces Ba^{2+} and there is no effect on superconductivity (Ishigaki, Izumi, Wada, Suzuki, Yaegashi, Asano, Yamaguchi & Tanaka, 1992). In contrast, Ca^{2+} substitution increases T_c significantly (Miyatake, Gotoh, Koshizuka & Tanaka, 1989; Knupfer, Nücker, Alexander, Romberg, Adelmann, Fink, Karpinski, Kaldis, Rusiecki & Jilek, 1991). NQR measurements had concluded (Mangelschots, Mali, Roos, Zimmermann, Brinkmann, Rusiecki, Karpinski, Kaldis & Jilek, 1990) that the Ca^{2+} ions also occupy barium sites.

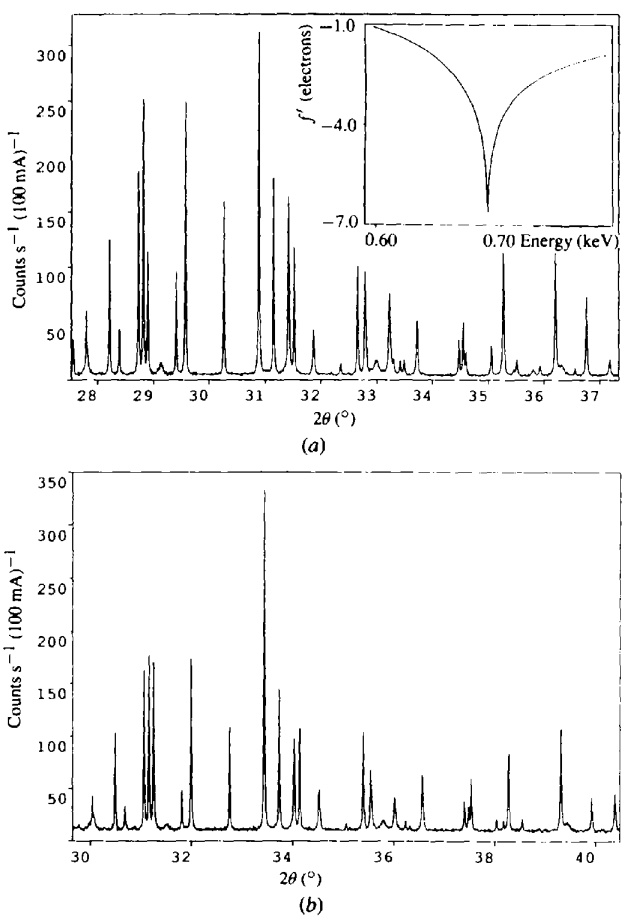

Fig. 12. High-resolution X-ray powder patterns of $Zn_3[Fe(CN)_6]_2$ taken (*a*) above and (*b*) below the Zn *K* edge, on the high-resolution powder diffractometer on beam line X7A (NSLS Brookhaven). Note the changes in relative intensities. The inset shows how f' changes with energy close to an edge (here, the Zr *K* edge).

At first sight, the relative X-ray scattering factors suggest this is an X-ray problem. Considering that the neutron scattering length of Ca is, at 4.70 fm, quite similar to that of Ba (5.07 fm), this would certainly seem not to be a neutron problem. However, determining the metal distribution from X-rays was hampered by severe texture effects. Neutron scattering was therefore attempted, after increasing the scattering contrast by substituting the Ca by ^{44}Ca, which has a scattering length of 1.42 fm which is very different from those of both Ba (5.07 fm) and Y (7.75 fm). As a result of this refinement, it became clear that, in disagreement with the interpretation of the NQR data, Ca was preferentially distributed into the Y rather than the Ba sites. Thus, the substitutional behaviour of the Sr and Ca ions is clearly different, each resulting in different effects on the superconducting transition temperature.

Any procedure which can enhance the scattering contrast between candidates for occupying a given site can potentially be exploited in solving site ordering problems. With the beam intensity and wavelength tunability available from synchrotron sources, we have the opportunity to use anomalous dispersion to vary atomic contrast by working at different wavelengths close to an absorption edge.

The inset to Fig. 12 shows the behaviour of the real part of the X-ray scattering factor f' close to an absorption edge. Depending on the edge and the element, a significant variation in the scattering factor can change the contrast of this element with respect to other atoms in the system, and hence gives us a handle with which to improve our ability to 'see' this particular element in the structure. The technique's exploitation has, however, so far been very limited, due probably in significant measure to the technical difficulties involved in performing an adequate stable experiment. The type of changes in relative intensities which can be seen in powder patterns taken with narrow monochromatic beams are illustrated for the microporous solid $Zn_3[Fe(CN)_6]_2$ in Fig. 12 taken above and at the Zn *K* edge (Cheetham & Wilkinson, 1991). We should, therefore, be able to exploit these differences in site-ordering problems.

An example of a successful application of the technique is the determination of the distribution of

Fe^{3+} and Ni^{2+} over the four crystallographically distinct octahedral sites in $FeNi_2BO_5$ (Perkins & Attfield, 1991). The scattering contrast between Fe^{3+} and Ni^{2+} is rather low, but by working close to the Fe *K* edge, the Fe scattering power could be reduced by *ca* 7 electrons, resulting in good contrast between the two metals. The results of this work indicated that the cation distribution is significantly non-random, and suggested that the cation distributions in these borates are determined by charge rather than size factors. The authors of the work also commented that the derived structural information using anomalous dispersion was as good as would be expected from a 'normal' X-ray powder measurement, and that even the B and O atoms were located with a precision greater than a recent single-crystal study. They also commented on the need to collect data over as wide a momentum transfer range as possible in order to minimize correlations between temperature factors and occupancies, as has been pointed out above.

One of the problems of using anomalous dispersion is the shift in the absorption edge – and hence of the f' values – with oxidation state. However, this oxidation state dependence also gives us an opportunity to study site-specific chemistry in powders by looking at distributions of different oxidation states between different sites. Work on gallium dichloride (Wilkinson, Cheetham & Cox, 1991) was able to refine the variation of the f' values of Ga^{I} and Ga^{III} with energy, giving results which are consistent with an oxidation state shift of up to 8 eV. Thus, anomalous dispersion should be able to be exploited to extract site-selective information on the distribution of different oxidation states in a powder material.

A successful example of such an experiment is the determination of the distribution of Eu^{2+} and Eu^{3+} between the three distinct cation sites in Eu_3O_4 (Attfield, 1990). By refining the f' and f'' values for the three cation sites, one of the sites was found to be electronically different from the other two, the differences being identified with Eu^{3+} in the Eu(1) and Eu(2) sites, with Eu^{2+} in the Eu(3) position. Similar work was also successfully performed on $EuSm_2O_4$, in which the cation and valence ordering were determined using anomalous scattering (Attfield, 1990).

Sample environment

The stress so far in this paper has been on the exploitation of improved neutron and X-ray sources and instrumentation, with particular emphasis on the potential of high-resolution powder studies made possible by significant advances in source intensity, combined with particular specific advantages of either probe. Increased source intensity also presents possibilities for data collection on 'standard size' samples in short times, with potential for studies of phase changes and chemical reactions *in situ*, measurements on small samples of particular importance in studies of new materials, and of working in restricted sample environments, for example under pressure and in reaction vessels.

The pressure variable is one which is only just beginning to be exploited to a significant extent, despite its potential value in both fundamental studies of elementary interactions between atoms, and in modifying the behaviour of potentially important materials, for example high-temperature superconductors. Because they are highly penetrating, and hence can pass through relatively thick-walled sample environment equipment, neutrons have been particularly exploited in high-pressure work. With the advent of pulsed spallation sources, in which white beams of neutrons can be effectively used, we have the opportunity to take a complete diffraction pattern at a fixed 90° scattering angle, which allows us to collimate out all the parasitic scattering due to the sample environment. Fig. 13(*a*)

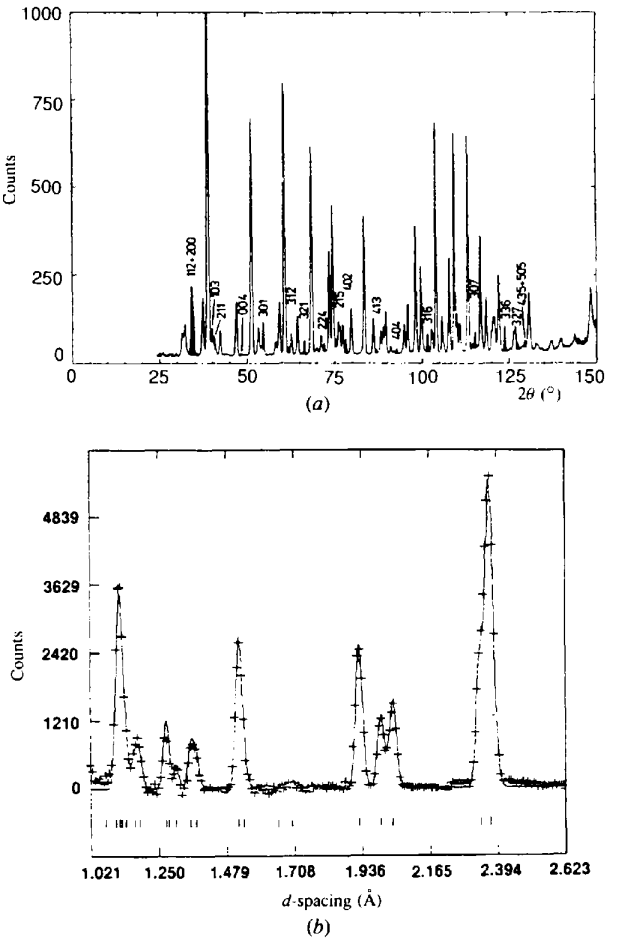

Fig. 13. Powder diffraction patterns of ice VIII taken on (*a*) the reactor neutron source at ILL and (*b*) the pulsed spallation neutron source IPNS. Only the labelled peaks in the upper figure originate from the sample. In the pulsed neutron pattern, the peaks from the pressure cell have been collimated out, exploiting the 90° fixed scattering geometry.

shows a powder pattern taken of ice VII in angle-dispersive mode on a reactor powder diffractometer (Kuhs, Finney, Vettier & Bliss, 1984). Although in this case the sample peaks identified could be extracted for structure refinement, the pattern is clearly dominated by the powder lines from the pressure cell. In contrast, data taken at 90° on the Argonne-pulsed source (Fig. 13*b*) illustrates quite dramatically how the scattering from the pressure cell can be completely collimated out, with a consequent improvement in data quality (Jorgensen, Beyerlin, Watanabe & Worlton, 1984).

Increasingly, neutron studies under pressures of up to *ca* 3.5 GPa are becoming almost routine, examples including work on the high-pressure ice phases (Jorgensen, Beyerlin, Watanabe & Worlton, 1984; Kuhs, Finney, Vettier & Bliss, 1984; Londono, Kuhs & Finney, 1993) and high-temperature superconductors (Takahashi, Jorgensen, Hunter, Hitterman, Shiyou, Izumi, Shimakawa, Kubo & Manako, 1992). However, one of the exciting recent developments is the pushing up to even higher pressures our ability to perform quantitative structure refinements. A major development of anvil cells on the ISIS-pulsed spallation source has reached pressures of over 25 GPa, and further developments can be expected both to higher pressures and in accessing these high pressures at lower temperatures. Data of sufficient quality for Rietveld refinement have been taken on ice VIII up to 10 GPa (Nelmes, Loveday, Wilson, Besson, Pruzan, Klotz, Hamel & Hull, 1993), from which the variation with pressure of the OD bond length has been determined. Very recent work has obtained data of refinable quality on ice VII up to 26 GPa (Klotz, Besson, Hamel, Nelmes, Loveday, Marshall & Wilson, 1995). We can confidently expect further exploitation of high pressure using neutrons, taking advantage of not only the 90° scattering geometry to reduce the background, but also the whole array of other advantages of neutrons as already discussed in application to powders.

In parallel, major advances are also being made in X-ray studies of powders under pressure. We have been able for many years to perform good X-ray work under pressure on relatively small samples using diamond anvil cells. However, as energy dispersive measurements using white beams can exploit – as in the neutron case – the limited scattering geometry imposed by anvil cells, much powder work has used energy-dispersive methods, with consequential reduction of the resolution obtainable due to the present energy resolution limitations of solid-state detectors. Over the past few years, however, there have been developments of anvil cells for angle-dispersive pressure work using synchrotrons (Nelmes, Hatton, McMahon, Piltz, Crain, Cernik & Bushnell-Wye, 1992). This work also takes advantage of advances in detector technology, in particular the use of image plates to improve in a major way the statistics available. Put simply, rather than just scan through a narrow line of the powder pattern as is normally done by an angle-dispersive detector scan, we can integrate round a significant fraction of the powder rings, resulting in major improvements in signal-to-background which enabled us to pick up important subtle effects that had previously been missed.

As an example, we consider InSb, a III–V semiconductor (Nelmes, McMahon, Hatton, Piltz & Crain, 1993). Despite over 30 years of work, significant uncertainties have remained about the crystal structures of the high pressure phases. These problems have now been clarified in high-pressure monochromatic work on the Daresbury synchrotron in which sequences of transitions involving four different structures have been observed and characterized. Fig. 14 shows the integrated profile of a pattern of the highest pressure phase obtained above *ca* 3 GPa. Two points might be noted. First, there are many weak peaks in the profile which cannot be explained on the expected orthorhombic unit cell. These turn out to be superlattice reflections which can be indexed on a $2a \times 3b \times 2c$ supercell, with systematic absences corresponding to a *B* face-centring. It is perhaps worth observing that without the very good signal-to-background ratio achieved in these experiments as a consequence of using image plates, these weak reflections would be extremely difficult, if not impossible, to observe. The second point concerns the changes in intensity observed when taking measurements of both the weak low-angle line and two of the superlattice reflections with incident X-ray energies both near (*n*) and far (*f*) from the In *K*-edge. Thus, we have another example of the exploitation of anomalous dispersion, which in this case allows us to conclude that the structure of this phase is site-ordered.

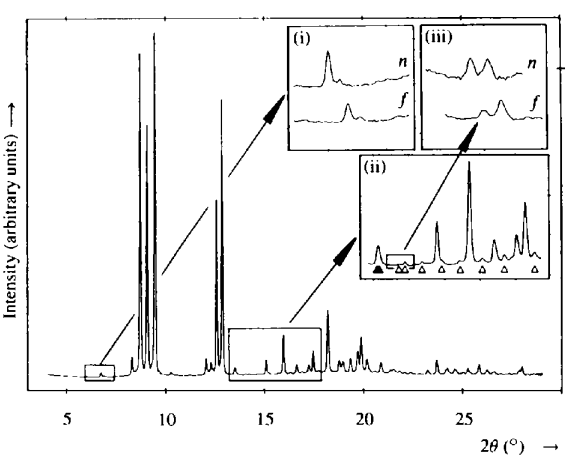

Fig. 14. The integrated profile of the highest pressure phase of InSb. Inset (i) shows a very weak low-angle line recorded with an X-ray wavelength far (*f*) from and near (*n*) to the In *K* edge. The enlargement in inset (ii) shows many weak superlattice lines marked Δ. Two of these are enlarged further in inset (iii), recorded far from and near to the In *K* edge. The image-plate technique enabled the important weak lines to be observed.

Diffuse scattering in single crystals

Although here the emphasis has largely been on powder methods, the advent of pulsed spallation neutron sources has opened up in such a major way the study of disorder in crystals that it is worth illustrating the type of work than can now be done in an area of potentially major materials science significance.

The great majority of crystal structure studies concentrate almost exclusively on the Bragg scattering. However, important information on defects that often dominate the electrical and mechanical properties of a crystalline material is found away from the Bragg peaks. Thus, if we are to understand defect structures, we need to look at data on the diffuse scattering that lies in the regions of reciprocal space between the Bragg spots.

There are many examples of diffuse scattering measurements made with both X-rays and neutrons. However, the amount of data that needs to be looked at is such that traditional angle-scanning techniques are extremely time-consuming. Using area detectors on pulsed spallation neutron sources, it is here that the white beam time-sorted Laue technique – in which we know from time-of-flight the wavelength of each detected neutron – is particularly powerful, making it possible to collect data sufficiently rapidly to make diffuse scattering measurements routine rather than exceptional.

An example of technological importance concerns solid electrolytes. In the case of halide fluorites, the substitution of trivalent dopant ions on to the cation sites results in a large reduction in the transition temperature above which ionic conductivity is observed in the system. Overall charge neutrality in the doped systems is maintained by the incorporation of excess ions into the anion sublattice. The topology of the defect clusters formed is, therefore, of some considerable interest.

Fig. 15(*a*) shows the measured coherent diffuse scattering in the (110) plane for $(Ca,Y)F_{2+x}$ (Hull & Wilson, 1992). We might note that to take such data on a reactor-based source we would have to scan the detector point-by-point through this reciprocal space plane, a procedure that would be much more time consuming. Even with the area detectors increasingly available on reactor sources, we would still be limited by selecting a single wavelength, whereas the time structure of the pulsed source permits the use of a wide spectrum of incident thermal neutrons. Using various defect models, the diffuse scattering can be calculated and compared with that observed experimentally. In this case, the best fit to the data (Fig. 15*b*) is obtained using the cuboctahedral defect cluster shown in Fig. 15(*c*), which can be formed as shown by conversion of six edge-sharing $(Ca,Y)F_8$ fluorite cubes into corner-sharing square antiprisms, as shown in the same figure.

A final example concerns the short-range hydrogen ordering in hexagonal ice, a phenomenon of fundamental importance to our understanding of hydrogen bonding. In this system, the water oxygens form a tetrahedral array with the hydrogens (or in this case deuterons) being disordered according to the Bernal–Fowler rules. These state that there are two deuterons close to each oxygen, but with only one deuteron between neighbouring oxygen centres. The distribution of hydrogens among the available sites is thus of interest.

Fig. 16(*a*) shows the diffuse scattering measured at 20 K in the orthorhombic *h*0*l* plane, while Fig. 16(*b*) shows that expected according to the Bernal–Fowler rules (Li, Nield, Ross, Whitworth, Wilson & Keen 1994). Although some of the features of the diffuse scattering are reproduced, there are clear discrepancies, in particular the strong streak of scattering along 60*l*. Thus, the simple application of the Bernal–Fowler rules is inadequate to explain the observed diffuse scattering, and attempts are needed to fit a model to experiment. One of these, in which all atoms are allowed to move under a reverse Monte Carlo procedure (Nield, 1995) is able to reproduce this 60*l* streak, as shown in Fig. 16(*c*). What the details of this fitted structure are remains to be analysed.

Summary: looking forward

This paper has attempted to look at some of the scientific developments that have been made possible by advances over the past 10 years or so in X-ray and neutron sources and instrumentation. The selection has been personal, concentrating on those areas I find particularly interesting and/or promising for the future. I have tried to show how increases in source brightness (spatial or temporal), or of 'effective' intensity (useful X-rays or neutrons measured) have allowed us to perform new science, either because of increases in resolution or through the ability to use smaller samples alone or in restricted environments. The exploitation of white beams – either by time-of-flight as in pulsed spallation neutron sources, or through X-ray tunability – has been an important feature of recent developments, as has our ability to cover wider energy and momentum transfer ranges. Throughout, I have concentrated on powder diffraction, although some reference has been made to particular kinds of single-crystal studies.

Where will we go from here?

Clearly, both X-rays and neutrons will continue to be used in refining more complex systems from powder data, and in studying more subtle effects and changes. We can already obtain in many systems single-crystal quality data from powders which allow us to perform quality refinements of thermal parameters, partial occupancies and disorder, and there is much scope for expansion of this kind of work. Although advances are to be expected in both X-ray and neutron refinements, the fall-off with scattering vector of the X-ray form factor

will tend to favour neutrons where a wide *d*-spacing range is required, and also where quantitatively precise refinements are of prime importance. The use of total diffraction measurements to look in detail, through the radial distribution function, at local interatomic distances is a technique deserving of wider application, although form factor and maximum **Q** limitations for X-rays are likely to direct its major usefulness towards the neutron front.

In site-ordering studies, both neutrons and X-rays could be increasingly exploited, taking note of the particular advantages of each when deciding which probe to use in a particular study. X-ray anomalous dispersion in this context is under-used: despite the technical problems associated with its use, it deserves much wider exploitation, and could result in significant progress in both site-ordering studies and site-selective chemistry.

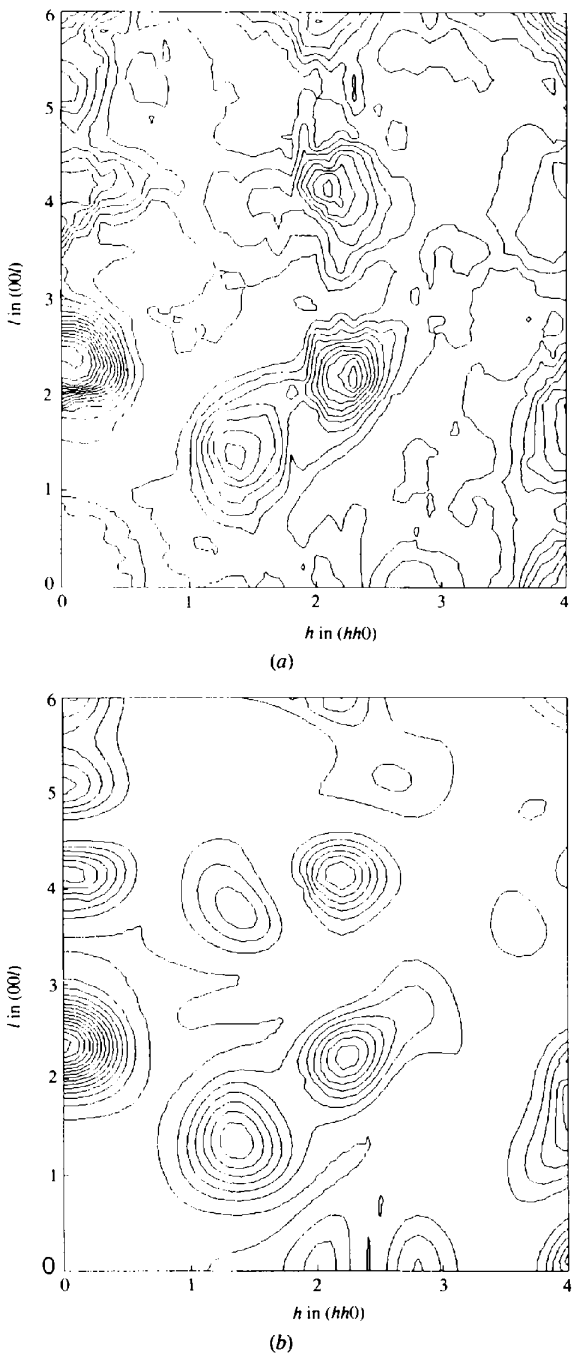

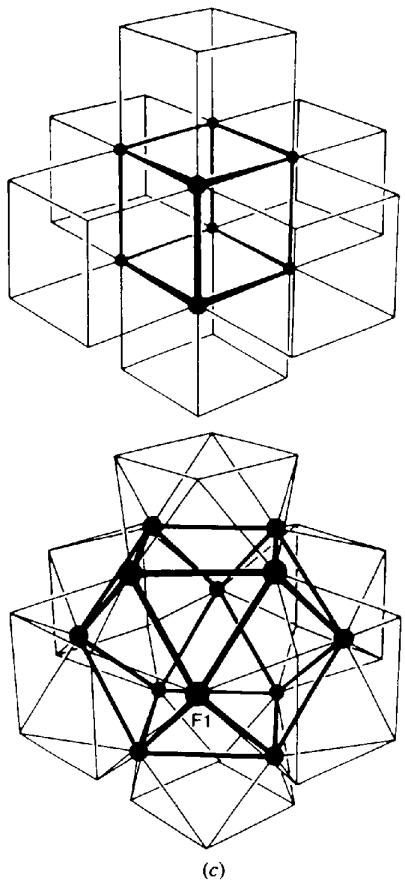

Fig. 15. (*a*) Measured and (*b*) calculated coherent diffuse scattering in the (110) plane for $(Ca_{0.94}Y_{0.06})F_{2.06}$. The calculated pattern assumed a random distribution of cuboctahedral defect clusters (see *c*).

Structure solution from powders is perhaps a problematical area. Much work has been done, although so far we have been successful – using either X-rays or neutrons – in only a relatively small number of cases. This is perhaps an area to watch, as present attempts to advance the technique come to be fully tested and further developed. There may be a limit to the size of structure that can be solved in this way, and although further improvement in attainable resolution is possible, the fact that we are approaching the useful limit set by particle size suggests that going to even higher instrumental resolution will not lead to a qualitative step forward. With appropriate development, however, we can be hopeful that *ab initio* structure determination from

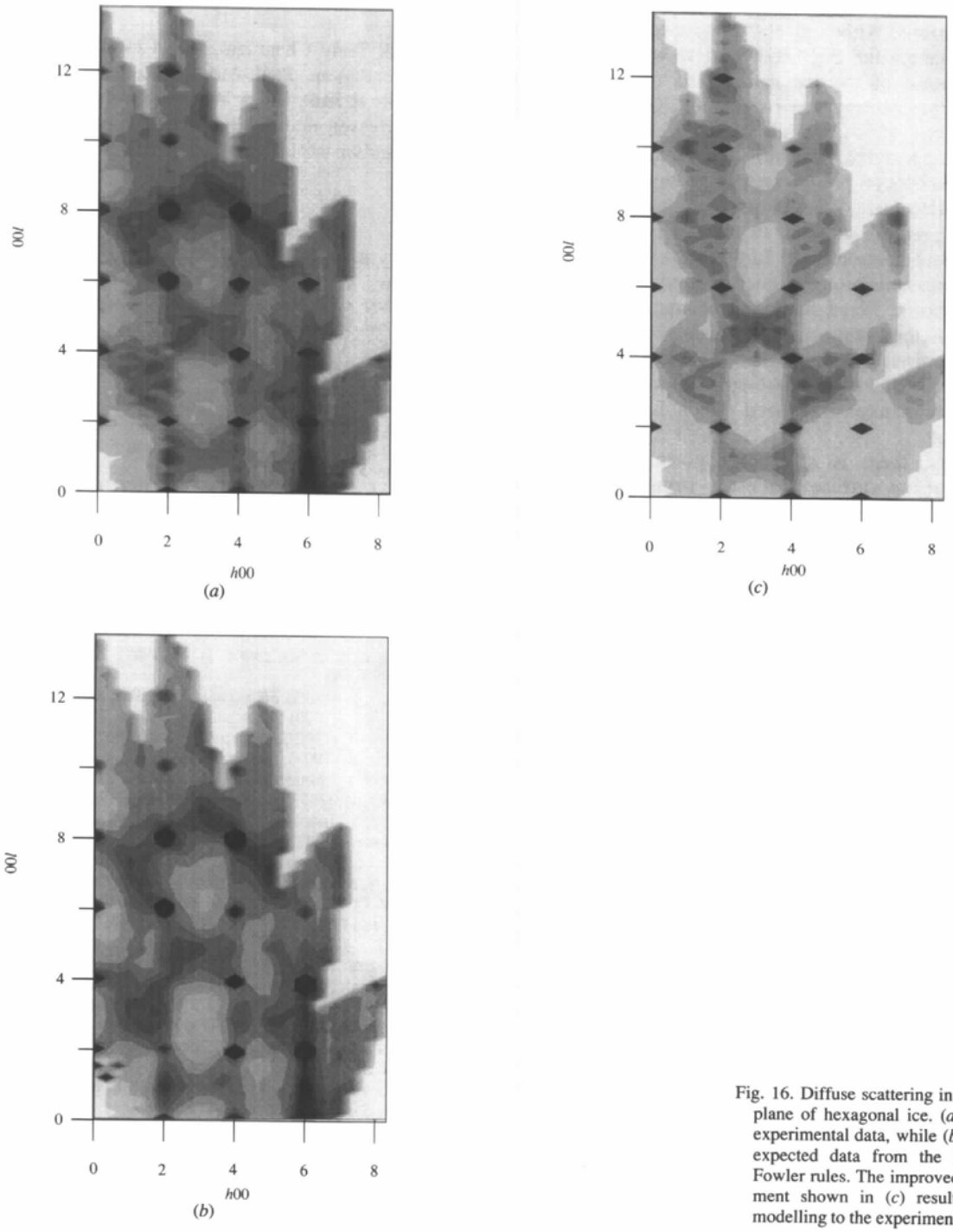

Fig. 16. Diffuse scattering in the $h0l$ plane of hexagonal ice. (*a*) is the experimental data, while (*b*) is the expected data from the Bernal–Fowler rules. The improved agreement shown in (*c*) results from modelling to the experimental data.

powders will become a generally useful technique for at least systems such as small organic molecules, and perhaps those of greater complexity.

Intensity also opens up major possibilities in studies of smaller systems. This can mean small amounts of new complex materials or shorter time-dependent experiments. Very short X-ray Laue experiments are already performed on single crystals and there are clear ways forward to reduce data collection times using both X-rays and neutrons. Although not mentioned above, we can already take a full diffraction pattern with neutrons in a single pulse of the Russian pulsed reactor at Dubna (Balagurov, Mironova, Novozchilov, Ostrovny, Simkin & Zlokazov, 1991), and initial studies using X-ray image plates suggest the possibility of rapid high-resolution measurements on present second-generation synchrotron sources (Bushnell-Wye, Finney & Wicks, 1995).

High pressure work is an area of potential for both X-rays and neutrons, and further developments to even higher pressures promise much for both fundamental and applied work. Fixed scattering geometry is particularly useful in improving signal-to-background, and in this respect pulsed spallation neutron sources have much to offer. Extension of high-pressure work to both low and high temperatures is a need which is being currently addressed.

Finally, there is significant potential for disorder studies using diffuse scattering from single crystals, taking advantage of the time-sorted Laue method made possible by pulsed neutrons. The fact that important material properties often depend critically on structural disorder suggests that such studies will be of increasing importance in the tailoring of material properties, in addition to producing results of fundamental importance.

Although 'complementary' is included in the title of this paper, I have largely refrained from discussing specific types of work in which X-rays and neutrons might be used on the same system to obtain information that might be considered in some way complementary. Rather, as stressed at the beginning, X-rays and neutrons see different things, and the most appropriate technique to use depends primarily on what we want to see. Moreover, both probes have their advantages and drawbacks, and these need to be considered in designing the most appropriate experiment. Furthermore, we should note that the balance of these advantages and disadvantages may be different depending on the sources of radiation available – what may be a disadvantage for a laboratory X-ray set may not weigh strongly if we have access to a third generation synchrotron source. A guiding rule could be to look for the most appropriate technique for a particular problem, taking these constraints into full account. It is perhaps all too easy to use the most easily available technique rather than the best one for a particular problem, an ease which it could be argued has resulted in both the use of X-rays, where neutrons would have been appropriate, and *vice versa*. Unfortunately, despite their wide and increasing usefulness, neutrons remain a scarce commodity, there being far fewer intense sources available with respect to the demand than is the case for synchrotron X-rays. Nevertheless, we should try to use the right probe for the problem we are trying to solve, which might be a laboratory X-ray source, a synchrotron, a reactor or pulsed spallation neutron source, or some other technique altogether.

I thank Tony Cheetham, Bob Cernik, Kevin Knight, Mike Henderson, Paul Attfield, Richard Ibberson, Bill David, Steve Hull, Chick Wilson, Richard Nelmes, Jean-Michel Besson and Vicky Nield for permission to use figures and/or unpublished material.

References

ATTFIELD, J. P. (1990). *Nature (London)*, **343**, 46–49.
BALAGUROV, A. M., MIRONOVA, G. M., NOVOZCHILOV, V. E., OSTROVNY, A. I., SIMKIN, V. G. & ZLOKAZOV, V. B. (1991). *J. Appl. Cryst.* **24**, 1009–1014.
BILLINGE, S. J. L. & EGAMI, T. (1992). In *Lattice Effects in High T_c Superconductors*, edited by Y. BAR-YAM. Singapore: World Scientific.
BOUQUIERE, J. P., FINNEY, J. L., LEHMANN, M. S., LINDLEY, P. F. & SAVAGE, H. F. J. (1993). *Acta Cryst.* B**49**, 79–89.
BOUQUIERE, J. P., FINNEY, J. L. & SAVAGE, H. F. J. (1994). *Acta Cryst.* B**50**, 566–578.
BUNGE, H. J., DAHMS, M. & BROKMEIER, H. G. (1989). *Cryst. Rev.* **2**, 67.
BUSHNELL-WYE, G., FINNEY, J. L. & WICKS, J. D. (1995). *Nucl. Inst. Methods*. In the press.
CARLILE, C. J. & FINNEY, J. L. (1991). *Physica B*, **174**, 451–469.
CERNIK, R. J., CHEETHAM, A. K., PROUT, C. K., WATKIN, D. J., WILKINSON, A. P. & WILLIS, B. T. M. (1991). *J. Appl. Cryst.* **24**, 222–226.
CHEETHAM, A. K. & WILKINSON, A. P. (1991). *J. Phys. Chem. Solids*, **52**, 1199–1208.
DAVID, W. I. F. (1989). *MRS Symp. Proc.* **166**, 41–54.
DAVID, W. I. F. (1990). *Nature (London)*, **346**, 731–734.
DAVID, W. I. F. (1992). *Physica B*, **180/181**, 567–574.
DAVID, W. I. F. (1993). Personal communication.
DAVID, W. I. F., IBBERSON, R. M., DENNIS, T. J. S., HARE, J. P. & PRASSIDES, K. (1992). *Europhys. Lett.* **18**, 219–225.
DAVID, W. I. F., IBBERSON, R. M. & MATSUO, T. (1993). *Proc. R. Soc. London Ser. A*, **442**, 129–146.
DAVID, W. I F., IBBERSON, R. M., MATTHEWMAN, J. C., PRASSIDES, K., DENNIS, T. J. S., HARE, J. P., KROTO, H. W., TAYLOR, R. & WALTON, D. R. M. (1991). *Nature (London)*, **353**, 147–149.
FINNEY, J. L. (1992). *Nucl. Inst. Methods B*, **68**, 451–458.
FISCHER, P., KALDIS, E., KARPINSKI, J., RUSIECKI, S., JILEK, E., TROUNOV, V. & HEWAT, A. W. (1993). *Physica C*, **205**, 259–265.
HODGKIN, D. C. (1984). *Proc. Ind. Acad. Sci. Chem. Sci.* **93**, 195–196.
HULL, S. & WILSON, C. C. (1992). *J. Solid State Chem.* **100**, 101–114.
IBBERSON, R. M. & PRAGER, M. (1995). *Acta Cryst.* B**51**, 71–76.
ISHIGAKI, T., IZUMI, F., WADA, T., SUZUKI, N., YAEGASHI, Y., ASANO, H., YAMAGUCHI, H. & TANAKA, S. (1992). *Physica C*, **191**, 441–449.
JEFFREY, G. A., RUBLE, J. R., MCMULLAN, R. K. & POPLE, J. A. (1987). *Proc. R. Soc. London Ser. A*, **414**, 47–57.
JORGENSEN, J. D., BEYERLIN, R. A., WATANABE, N. & WORLTON, T. G. (1984). *J. Chem. Phys.* **81**, 3211–3214.
KLOTZ, S., BESSON, J. M., HAMEL, G., NELMES, R. J., LOVEDAY, J. S., MARSHALL, W. G. & WILSON, R. M. (1995). *Appl. Phys. Lett.* **66**, 1735–1737.

KNIGHT, K. S., HENDERSON, C. M. B. & WOOD, B. J. (1995). *Am. Mineral.* Submitted.

KNUPFER, M., NÜCKER, N., ALEXANDER, M., ROMBERG, H., ADELMANN, P., FINK, J., KARPINSKI, J., KALDIS, E., RUSIECKI, S. & JILEK, E. (1991). *Physica C*, **182**, 62–66.

KUHS, W. F., FINNEY, J. L., VETTIER, C. & BLISS, D. V. (1984). *J. Chem. Phys.* **81**, 3612–3623.

LEBAIL, A., DUROY, H. & FOURQUET, J. L. (1988). *Mat. Res. Bull.* **23**, 447–452.

LENHERT, P. G. (1968). *Proc. R. Soc. London Ser. A*, **303**, 45–84.

LENHERT, P. G. & HODGKIN, D. C. (1961). *Nature (London)*, **192**, 937–938.

LI, J. C., NIELD, V. M., ROSS, D. K., WHITWORTH, R. W., WILSON, C. C. & KEEN, D. A. (1994). *Philos. Mag. B*, **69**, 1173–1181.

LONDONO, J. D., KUHS, W. F. & FINNEY, J. L. (1993). *J. Chem. Phys.* **98**, 4878–4888.

LONSDALE, K. (1929). *Proc. R. Soc. London Ser. A*, **123**, 494–515.

LÜTHI, H. P. & ALMLÖF, J. (1987). *Chem. Phys. Lett.* **135**, 357–360.

MANGELSCHOTS, I., MALI, M., ROOS, J., ZIMMERMANN, H., BRINKMANN, S., RUSIECKI, S., KARPINSKI, J., KALDIS, E. & JILEK, E. (1990). *Physica C*, **172**, 57–62.

MCCUSKER, L. B. (1988). *J. Appl. Cryst.* **21**, 305–310.

MCCUSKER, L. B., BAERLOCHER, CH., JAHN, E. & BÜLOW, M. (1991). *Zeolites*, **11**, 308–311.

MIYATAKE, T., GOTOH, S., KOSHIZUKA, N. & TANAKA, S. (1989). *Nature (London)*, **341**, 41–42.

MOORE, F. M., WILLIS, B. T. M. & HODGKIN, D. C. (1967). *Nature (London)*, **214**, 129–133.

NELMES, R. J., HATTON, P. D., MCMAHON, M. I., PILTZ, R. O., CRAIN, J., CERNIK, R. J. & BUSHNELL-WYE, G. (1992). *Rev. Sci. Instrum.* **63**, 1039–1042.

NELMES, R. J., LOVEDAY, J. S., WILSON, R. M., BESSON, J. M., PRUZAN, P., KLOTZ, S., HAMEL, G. & HULL, S. (1993). *Phys. Rev. Lett.* **71**, 1192–1195.

NELMES, R. J., MCMAHON, M. I., HATTON, P. D., PILTZ, R. O. & CRAIN, J. (1993). *Jpn. J. Appl. Phys.* **32**, Suppl. 32-1, 1–5.

NIELD, V. M. (1995). *Nucl. Inst. Methods A*, **354**, 30–37.

PAWLEY, G. S. (1981). *J. Appl. Cryst.* **14**, 357–361.

PERKINS, D. A. & ATTFIELD, J. P. (1991). *J. Chem. Soc. Chem. Commun.* pp. 229–231.

SAVAGE, H. F. J. (1986*a*). *Biophys. J.* **50**, 947–980.

SAVAGE, H. F. J. (1986*b*). In *Water Sciences Reviews*, edited by F. FRANKS, Vol. 2, pp. 67–148. Cambridge Univ. Press.

SAVAGE, H. F. J. & FINNEY, J. L. (1986). *Nature (London)*, **322**, 717–720.

SAVAGE, H. F. J., LINDLEY, P. F., FINNEY, J. L. & TIMMINS, P. A. (1987). *Acta Cryst.* B**43**, 280–295.

TAKAHASHI, H., JORGENSEN, J. D., HUNTER, B. A., HITTERMAN, R. L., SHIYOU, P., IZUMI, F., SHIMAKAWA, Y., KUBO, Y. & MANAKO, T. (1992). *Physica C*, **191**, 248–254.

WEISS, E., CORBELIN, S., COCKCROFT, J. K. & FITCH, A. N. (1990*a*). *Angew. Chem. Int. Ed. Engl.* **28**, 650–652.

WEISS, E., CORBELIN, S., COCKCROFT, J. K. & FITCH, A. N. (1990*b*). *Chem. Ber.* **123**, 1629–1634.

WILKINSON, A. P., CHEETHAM, A. K. & COX, D. E. (1991). *Acta Cryst.* B**47**, 155–161.

WINDSOR, C. G. (1981). *Pulsed Neutron Scattering*. London: Taylor & Francis.

YOUNG, R. A. (1993). *The Rietveld Method*. Oxford Univ. Press.